CALIFORNIA STATE UNIVERSITY NORTHRIDGE

INSULIN-STIMULATED COMPARTMENTALIZATION AND ACTIVATION OF aPKCζ/λ IN OBESE ZUCKER RAT SKELETAL MUSCLE

A thesis submitted in partial fulfillment of the requirements

For the degree of Masters of Science

in Biology

By

Tania Yadira Figueroa

December 2009

The Thesis of Tania Yadira Figueroa is approved:

Ben B. Yaspelkis III, Ph.D.	Date
Cindy S. Maloke Ph.D.	Date
Randy W. Cohen, Ph.D., Chair	Date

California State University, Northridge

ACKNOWLEDGEMENTS

I would like to thank my thesis advisor Dr. Ben Yaspelkis III, for introducing me to the field of exercise physiology and providing me with guidance throughout this thesis and beyond.

I would also like to thank my thesis committee members Dr. Randy Cohen and Dr. Cindy Malone.

I extend a special thanks to the members of the Exercise Biochemistry Laboratory: Mohammad Tabek Bakir, Ilya Kvasha, Misato Saito, Neal Washburn, and Jason Ue. Each member contributed to the completion of this thesis. Their support at the bench and friendship outside the lab has been greatly appreciated.

Thank you to my husband, Jorge De Santiago, my rock and my number one fan. Without him this would have never been possible.

A special thanks to my mother, Aurelia Figueroa, my hero, for her continuous support and unconditional love.

Finally, I would like to declare my faith in our Lord Jesus Christ because through him all things are possible.

TABLE OF CONTENTS

ABSTRACT

INSULIN-STIMULATED COMPARTMENTALIZATION AND ACTIVATION OF aPKCζ/λ IN OBESE ZUCKER RAT SKELETAL MUSCLE

By

Tania Yadira Figueroa

Master of Science in Biology

In the obese Zucker rat, a genetic model of insulin resistance, it is well established that rates of insulin-stimulated skeletal muscle glucose transport are impaired due to an inability to appropriately translocate the glucose transporter (GLUT4) to the plasma membrane. However, it has not been extensively investigated if the reduced plasma membrane GLUT4 protein concentration results from impairments in the activation and/or compartmentalization of the distal components of the insulin signaling cascade in this rodent model of insulin resistance. Sixteen male lean (LZR, n=8) and obese (OZR, n=8) Zucker rats that were 4 weeks of age were provided normal rat chow *ad libitum* for 4 weeks and then subjected to hindlimb perfusions. In the absence of insulin, plasma membrane aPKCζ/λ protein concentration was reduced in the OZR compared to the LZR. In response to insulin stimulation, the OZR exhibited decreased translocation of aPKCζ/λ to the plasma membrane, as well as exhibiting decreased activation of aPKCζ/λ in both the cytosolic and plasma membrane fractions. The decreased insulin-stimulated activation and translocation of aPKCζ/λ appeared to be due to insulin-stimulated activation of PI3-K being reduced in the OZR. This in turn reduced the activation and appropriate compartmentalization of aPKCζ/λ in the skeletal muscle of the OZR and it is likely that this impairment in the distal component of the insulin signaling cascade partially accounts for why plasma membrane GLUT4 protein concentration and rates of glucose

transport were decreased in the skeletal muscle of the OZR compared to the LZR.

INTRODUCTION

The high-fat fed rodent model has been widely used to study how environmental factors, specifically diet, contribute to the development of insulin resistance in rat skeletal muscle (13, 18, 23, 24, 26, 28). It is suggested that insulin resistance in high-fat fed animals is a result of alterations in the insulin signaling cascade beginning at phosphatidylinositol 3' kinase (PI3-K) and including distal components of the cascade (1, 10, 14, 18, 19, 23). Such alterations decrease skeletal muscle insulin-stimulated GLUT4 translocation to the plasma membrane and impair glucose uptake. Specifically, our lab has found reductions in IRS-1 associated PI3-K activity, GLUT4 protein concentration, and insulin-stimulated plasma membrane-associated aPKCζ/λ protein concentration and activity (13, 18, 23, 26) in skeletal muscle of high-fat fed animals.

It has been shown that aPKCζ/λ activation is necessary for insulin-stimulated GLUT4 translocation and glucose uptake; functions that are largely impaired in insulin resistant tissues (2, 4, 5, 11, 12, 17, 24). Of interest, Etgen et al. (11) found that *in vivo* adenoviral delivery of aPKC stimulated glucose transport in rat skeletal muscle and Kotani et al. (13) reported that aPKC is required for insulin-stimulated glucose uptake in 3T3-L1 adipocytes. A more recent investigation by Bandyopadhyay et al. (3) found that insulin-stimulated glucose transport is impaired in embryonic cell lines and adipocytes in which both alleles that encode for aPKC have been knocked out. The same study found that the impairments were diminished by the adenoviral-mediated expression of aPKC in the cells (3).

The impairments in the skeletal muscle insulin signaling cascade attributed to effects of a high-fat diet have also been found in the skeletal muscle of the obese Zucker

rat; which has been studied as a genetic model of insulin resistance (1, 8, 9, 10, 15, 16, 22). Skeletal muscle insulin resistance occurring in the obese Zucker rat is largely a result of the inability of insulin to incorporate glucose transporters to the plasma membrane. Similar to high-fat fed rodents, this impairment in insulin signaling begins at PI3-K as evidenced by decreased IRS-1 associated PI3-K activity in skeletal muscle of the obese Zucker rat (1). Additionally, plasma membrane GLUT4 protein concentration is decreased in obese Zucker rats (7, 16), a phenomenon that is also present in high-fat fed rodents. Apart from these findings, little else is known about the other components of the insulin signaling cascade in the Zucker rat. Taking into account the similar alterations in proximal components of the insulin signaling cascade found in both rodent models, it is possible that these models may also share alterations in distal components of the cascade. Numerous studies have found that aPKCζ/λ protein concentration and activation are decreased in the high-fat fed rodent (9, 10, 14, 21); however similar impairments of aPKCζ/λ in Zucker skeletal muscle have not been well elucidated. Therefore the aim of the present investigation was to measure aPKCζ/λ compartmentalization and activation in skeletal muscle of the genetically obese Zucker rat.

METHODS

Experimental Design. Sixteen male Zucker rats (n=8 obese, n=8 lean) approximately four weeks of age were obtained from Charles River Laboratories (Wilmington, MA). The animals were fed normal rat chow (LabDiet #5001, PMI Nutrition International, LLC; Brentwood, MO) and water *ad libitum* for 4 wk. Animals were housed 2 per cage according to their type (lean/lean, obese/obese) in a temperature-controlled environment at 21° C with an artificial 12-12 h light-dark cycle.

All experimental procedures were approved by the Institutional Animal Care and Use Committee at California State University, Northridge and conformed to the guidelines for the use of laboratory animals published by the U.S. Department of Health and Human Services.

Hindlimb Perfusions. Following the 4 wk feeding period all animals were fasted for 8-12 h and prepared for hindlimb perfusions. Animals were anesthetized with an intraperitoneal injection of sodium pentobarbital (6.5 mg·100 g body wt^{-1}) and surgically prepared for hindlimb perfusion as previously described by Ruderman et al. (44) and modified by Ivy et al. (27). Following surgical preparation the iliac artery was tied off and the red quadriceps (RQ) muscle on the right hindlimb was collected, freeze clamped in liquid nitrogen and stored at -80° C for later analysis as basal tissue. Immediately following the removal of the right red quadriceps, catheters were inserted into the abdominal aorta and vena cava and the animals were sacrificed via an intracardiac injection of pentobarbital as the left hindlimb was washed out with 30mL of Krebs-Henseleit buffer (KHB) (pH 7.55). The catheters were placed in line with a non-recirculating perfusion system and the right hindlimb was allowed to stabilize during a 5

min washout period. The perfusate was continuously gassed with a mixture of 95% O_2-5% CO_2 and warmed to 37° C. Perfusate flow rate was set at 7.5 $mL \cdot min^{-1}$ during the stabilization and subsequent perfusion during which rates of glucose transport were determined.

Perfusions were performed in the presence of 500$\mu U \cdot mL^{-1}$ insulin for all animals. The basic perfusate medium consisted of 30% washed time-expired human erythrocytes (Ogden Medical Center, Ogden, UT), KHB, 4% dialysed bovine serum albumin (BSA) (EQUITECH-BIO, INC., Kerrville, TX) and 0.2 mM pyruvate. The hindlimbs were washed out with perfusate containing 1 mM glucose for 5 min in preparation for the measurements of glucose transport. Glucose transport was measured over an 8 min period using an 8 mM concentration of non-metabolized glucose analogue 3-O-methylglucose (3MG) (32 μCi 3-[^{3}H] $MG \cdot mM^{-1}$, PerkinElmer Life Sciences, Boston, MA) and 2mM mannitol (60 μCi-[^{14}C] $mannitol \cdot mM^{-1}$, Perkin Elmer Life Sciences). Rates of insulin-stimulated skeletal muscle 3-MG transport were calculated as previously described (38, 57, 60). Immediately after the transport period portions of the RQ were excised from the right hindlimb, blotted on gauze dampened with cold KHB, freeze clamped in liquid N_2 and stored at -80° C for later analysis as insulin-stimulated tissue.

Muscle Lysate Preparation. RQ muscle samples were weighed and homogenized 1:10 in homogenization buffer (HB) that contained 50mM HEPES, 150mM NaCl, 200 mM sodium pyrophosphate, 20mM β-glycerophosphate, 20mM NaF, 2mM sodium vanadate, 20mM EDTA, 1% IGPAL, 10% glycerol, 2mM phenylmethylsufonylfluoride, 1mM $MgCl_2$, 1 mM $CaCl_2$, 10$\mu g \cdot mL^{-1}$ leupeptin, and 10 $\mu g \cdot mL^{-1}$ aprotinin. Muscles were homogenized on ice using a PT 2100 polytron homogenizer (Kinematica, Littau/Luzern,

Switzerland) and centrifuged at 18,300 x *g* for 15 min at 4° C (Micromax RF, International Equipment Co., Needham Heights, MA). The supernatant was collected, labeled as lysate and quantified for protein content by the Bradford Method (11) using a Benchmark microplate reader (BioRad, Richmond, CA).

Plasma Membrane Fractionation. Plasma membrane fractions were prepared from RQ as described previously (40). Briefly, a portion of the RQ was homogenized using a PT 2100 polytron homogenizer (Kinematica) in 8x (wt/vol) ice-cold buffer containing 20mM HEPES (pH 7.4), 2mM EGTA, 50mM β-glycerophosphate, 1mM dithiothreitol, 1mM Na_3VO_4, 10% glycerol, 3 mM benzamidine, 10 μM pepstain A, and 1mM phenylmethylsulfonylfluoride. The homogenate was centrifuged at 100,000 x *g* for 30 min at 4° C in a Beckman Coulter Optima L-100 XP Ultracentrifuge (Beckman Coulter Inc., Fullerton, CA) using a T50.2i rotor. The supernatant was collected as the cytosolic fraction. The pellet was resuspended in 4x (wt/vol) ice-cold HB with 1% Triton X added. The resuspended pellet was then centrifuged at 15,000 x *g* for 10 min at 4° C and the supernatant was collected as the plasma membrane fraction.

IRS-1 Associated PI3- kinase Activity. IRS-1 associated activity was determined as we have described previously (47). Two hundred micrograms of protein lysate was immunoprecipitated with 4 μg of anti-IRS-1 antibody (Cat# 06-248, Millipore, Billerica, MA) and HB for 2 hours at 4° C. Following 1 h of separation the TLC plate was dried, exposed to a storage phosphor screen (Eastman Kodak Company, Rochester, NY) and scanned with a phosphor imager (Personal Molecular Imager FX System, BioRad). The image was imported into a Macintosh G4 computer and quantified using Quantity One

analysis software (BioRad). Kinase activity was calculated as a percentage of an insulin-stimulated muscle standard run on each TLC plate.

Western Blotting. Western blot analysis for aPKCζ/λ and GLUT4 was determined in the plasma membrane and cytosolic fractions of RQ muscle samples. Samples were combined (1:1) with Laemmli sample buffer and heated at 100° C for 5 minutes. Two hundred micrograms of muscle protein were subjected to sodium dodecyl sulfate-polyacrylamide gel electrophoresis (SDS-PAGE) run under reducing conditions on 10% resolving gels using a Mini-Protean III dual slab cell (BioRad). Resolved gels were equilibrated in a Bjerrum and Schafer-Nielson Transfer Buffer for 30 min. Resolved proteins were then transferred to Polyvinylidene difluoride (PVDF) membranes using a semidry-transfer unit (20V for 20 min). The membranes were blocked in 5% non-fat dry milk-Tween 20 tris buffered saline (NFDM-TTBS) blocking solution and incubated with either affinity purified rabbit polyclonal anti-aPKCζ (Cat#sc-216, Santa Cruz Biotechnology (SCBT), Santa Cruz, CA) or anti-GLUT4 (donated by Dr. Samuel W. Cushman, National Institute of Diabetes and Digestive and Kidney Diseases, Bethesda, MD) followed by incubation with a species specific secondary antibody conjugated to horse radish peroxidase (HRP). Antibody binding was visualized using enhanced chemiluminescence (ECL) in accordance to the manufacturer's instructions. Images were captured using a ChemiDoc system (BioRad) equipped with a charged coupled device camera and saved to a Macintosh G4 computer. Protein bands were quantified as a percentage of a standard muscle run on each gel using Quantity One analysis software (BioRad).

a*PKCζ/λ Kinase Activity Assay.* Sixty microliters of Pro-A slurry was incubated with 5 μg of anti-PKCζ (Cat# sc-216, SCBT) overnight at 4° C with rotation. Following an overnight incubation 500 μg of either cytosolic or plasma membrane protein samples were added to the immunocomplexes and placed on rotation for 2 h at 4° C. The immunocomplexes were then washed by using the same protocol as described for immunoprecipitation (45). After the final wash the supernatant was completely removed from the Pro-A beads. The kinase reaction was started by adding 30 μL of PKC reaction buffer, 5 μL myelin basic protein (M8-184, Sigma-Aldrich, St. Louis, MO) and 0.5 μL of [γ-^{32}P] ATP (PerkinElmer Life Sciences) to each sample. The samples were vortexed periodically while incubating for 12 min at 37° C. Reactions were terminated by the addition of Laemmli buffer (1:1). For analysis, seven microliters of sample were subjected to SDS-PAGE run under reducing conditions on a 20% Tris-tricine resolving gel. After electrophoresis the gels were wrapped in plastic wrap and exposed to a phosphor screen (Eastman Kodak Company) for 8 h. Images were captured and quantified as described above.

Statistical Analysis. An analysis of variance (ANOVA) was used on all variables to determine whether significant differences existed between groups. When a significant *F*-ratio was obtained, a Tukey HSD post hoc test was used to identify statistically significant differences ($p<0.05$) among the means. Statistical analyses were performed using JMP software (SAS Institute Inc., Cary, NC) and all values are expressed as means ± SE.

RESULTS

Glucose Transport. Rates of insulin-stimulated 3-O methylglucose (3-MG) transport in obese Zucker rats were significantly ($p<0.05$) decreased when compared to lean littermates in both the RG (lean: 2.83±0.60 μmol $g^{-1}\cdot h^{-1}$ vs. obese: 0.90±0.18 μmol $g^{-1}\cdot h^{-1}$) and RQ (obese: 3.91±0.65 μmol $g^{-1}\cdot h^{-1}$ vs. obese: 1.32±0.35 μmol $g^{-1}\cdot h^{-1}$).

IRS-1 Associated PI3-K Activity. In the absence of insulin IRS-1 associated PI3-K activity was similar among lean and obese Zucker rats (Fig. 1). Under insulin-stimulated conditions PI3-K activity was significantly decreased ($p<0.05$) in the obese Zucker rat when compared to lean littermates.

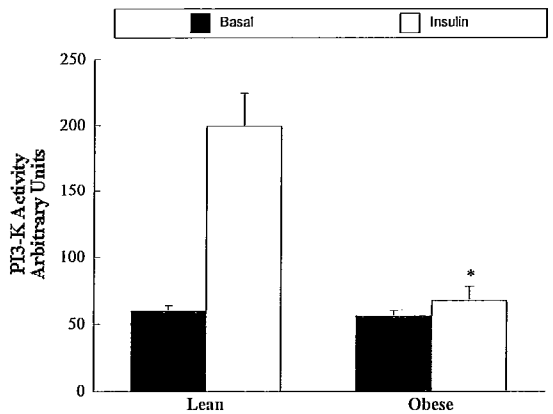

Figure 1. IRS-1 associated PI3-K activity obtained from lean and obese animals. *, Significantly different from group lean condition ($p< 0.05$). Values are expressed as means ± SE.

GLUT4 Protein Concentration. Cytosolic GLUT4 protein concentration was significantly lower ($p<0.05$) in obese Zucker rats in both basal and insulin-stimulated conditions when compared to lean littermates (Fig. 2A). Cytosolic GLUT4 protein concentration of both lean and obese Zuckers fell below basal levels in insulin-stimulated conditions. In the absence of insulin plasma membrane GLUT4 protein concentration was similar in lean and obese Zucker rats (Fig 2B). Under insulin-stimulated conditions plasma membrane GLUT4 protein concentration increased above basal levels in both

groups, however, the increase was significantly lower ($p<0.05$) in obese Zucker rats when compared to lean littermates.

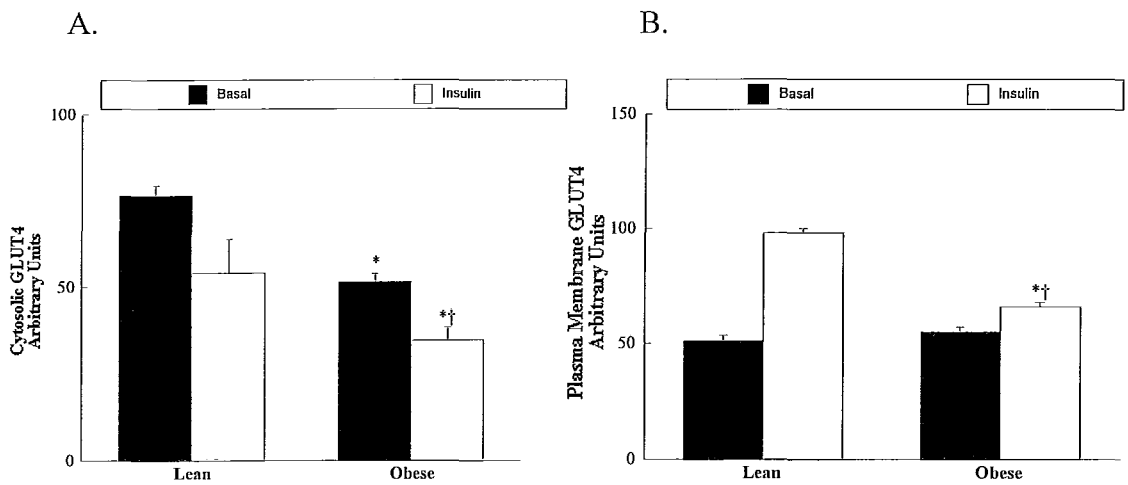

Figure 2. Cytosolic glucose transporter 4 (GLUT4) protein concentration (A) and plasma membrane GLUT4 protein concentration (B) obtained from lean and obese animals. *, Significantly different from group lean condition ($p<0.05$). †, Significantly different from obese basal condition ($p<0.05$). Values are expressed as means ± SE.

aPKCζ/λ Protein Concentration. In the absence of insulin cytosolic aPKCζ (Fig. 3A) and aPKCλ (Fig. 3B) protein concentrations were similar in obese and lean animals. Under insulin-stimulated conditions cytosolic aPKCζ and aPKCλ protein concentrations were significantly decreased ($p<0.05$) in obese Zucker rats when compared to lean littermates. In the absence of insulin plasma membrane-associated aPKCζ (Fig. 4A) and aPKCλ (Fig. 4B) protein concentrations were significantly reduced in obese Zucker rats compared to lean littermates. Under insulin-stimulated conditions plasma membrane-associated aPKCζ and aPKCλ were significantly reduced ($p<0.05$) in obese Zucker rats when compared to lean littermates.

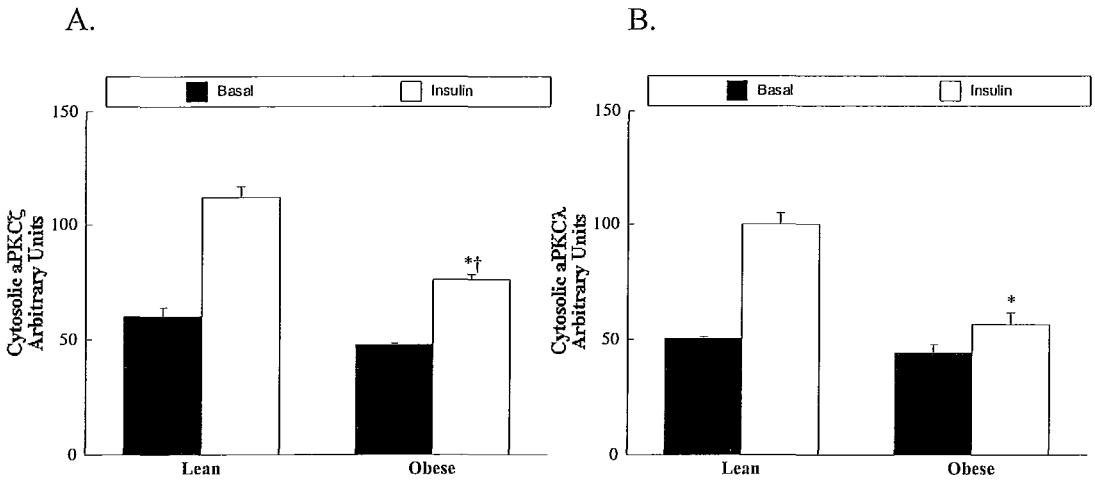

Figure 3. Cytosolic aPKCζ protein concentration (A) and cytosolic aPKCλ protein concentration (B) obtained from lean and obese animals. *, Significantly different from group lean condition ($p<0.05$). †, Significantly different from obese basal condition ($p<0.05$). Values are expressed as means ± SE.

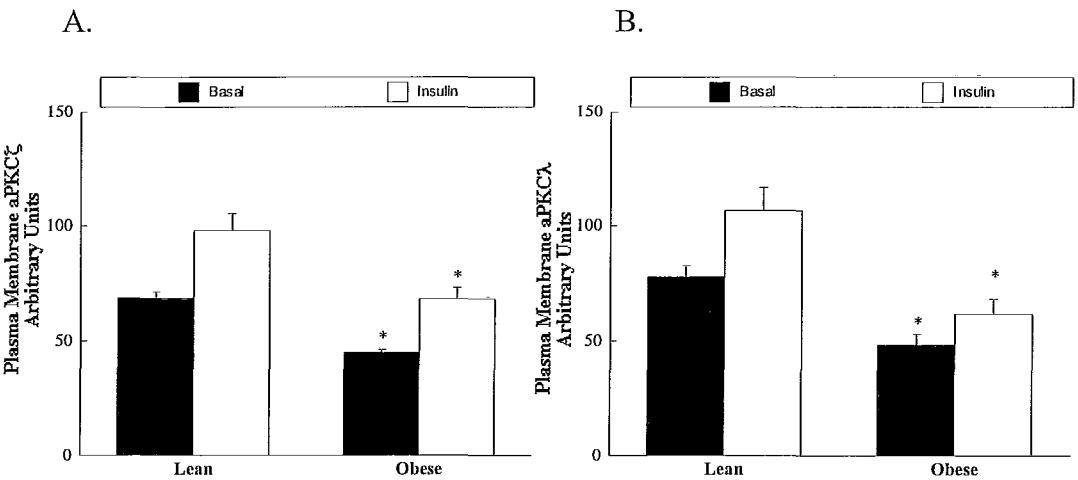

Figure 4. Plasma membrane aPKCζ protein concentration (A) and plasma membrane aPKCλ protein concentration (B) obtained from lean and obese animals. *, Significantly different from group lean condition ($p<0.05$). Values are expressed as means ± SE.

aPKCζ/λ Kinase Activity. In the absence of insulin cytosolic aPKCζ/λ activity was similar among lean and obese Zucker rats (Fig. 5A). Under insulin-stimulated conditions there was a significant reduction ($p<0.05$) in cytosolic aPKCζ/λ activity in obese Zucker rats when compared to lean littermates. In the absence of insulin plasma membrane

aPKCζ/λ activity was similar among lean and obese Zucker rats (Fig. 5B). Under insulin-stimulated conditions there was a significant decrease ($p<0.05$) in plasma membrane aPKCζ/λ activity in obese Zucker rats when compared to lean littermates.

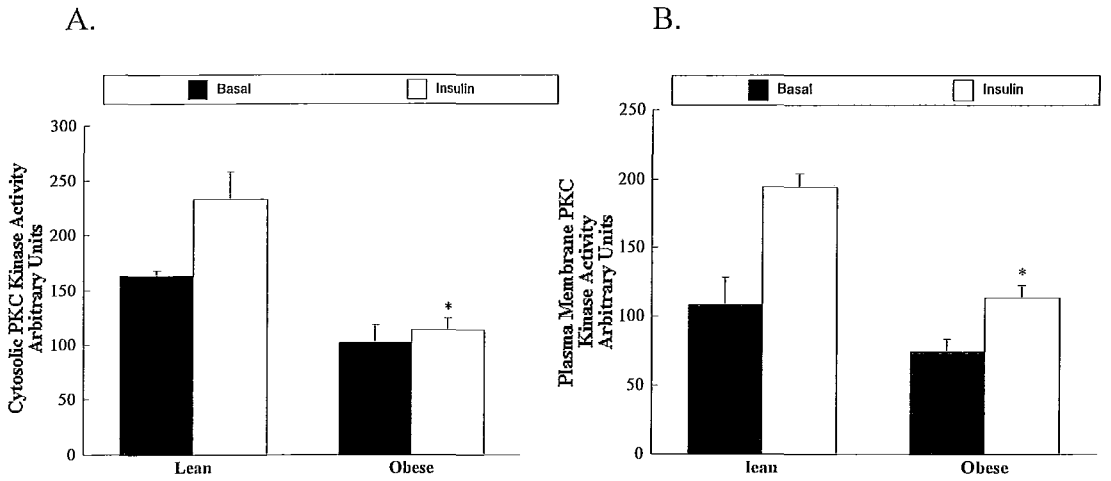

Figure 5. Cytosolic aPKCζ/λ activity (A) and plasma membrane aPKCζ/λ activity (B) obtained from lean and obese animals. *, Significantly different from group lean condition ($p<0.05$). Values are expressed as means ± SE.

DISCUSSION

The obese Zucker rat has been widely used to study insulin resistance and obesity (1, 5, 10, 12, 13, 16, 17, 18, 32, 46). It has been shown that insulin resistance in the skeletal muscle of the obese Zucker rat is associated with abnormalities in glucose uptake including alterations in insulin binding, reduced insulin receptor number and reduced glucose metabolism (16, 17, 36). Although there have been several studies that have evaluated proximal components of the insulin signaling cascade in the skeletal muscle of the Zucker rat (1, 14, 17, 55), there is a dearth of research on the distal components of the insulin signaling cascade. Christ et al. (16) have suggested that a reduction in PI3-K activity in the obese Zucker rat results in impairments to the insulin signaling cascade eventually resulting in a reduction in glucose uptake. We have found that a reduction in insulin-stimulated PI3-K activity in the skeletal muscle of high-fat fed rats leads to alterations in compartmentalization and activity of distal components of the insulin signaling cascade, specifically Akt2 and aPKCζ/λ (9, 24, 38, 47), resulting in a reduction in glucose transport. Thus, it was of interest to investigate whether insulin-stimulated aPKCζ/λ protein compartmentalization and activity are also altered in the skeletal muscle of the obese Zucker rat that would contribute to reduced rates of glucose transport.

In agreement with a number of previous investigations (10, 11, 12, 13, 16, 17, 19, 36, 46), we found that the obese Zucker rat exhibits a significant reduction in insulin-stimulated rates of 3-MG transport compared to lean counterparts. Concurrently, we found a significant reduction in insulin-stimulated plasma membrane GLUT4 protein concentration in the skeletal muscle of the obese Zucker rat. It has been suggested in the obese Zucker rat that alterations in the glucose transport seem to be the main cause of

insulin resistance (12, 13, 36). It has been shown that insufficient activation of PI3-K results in a reduction of the activity of distal components of the insulin signaling cascade (8, 26, 30, 34, 35, 49, 50, 54). Therefore, our initial measurement was directed at the insulin-stimulated activation of PI3-K in the obese Zucker rat. The obese Zucker rat exhibited a significant reduction in insulin-stimulated IRS-1 associated PI3-K activity when compared to lean littermates. This observation parallels that of Christ et al. (16), who found a reduction in insulin-stimulated PI3-K activity in the obese Zucker rat, and raises the possibility that insulin-stimulated activation of distal components of the insulin signaling cascade would also be affected in the skeletal muscle of the obese Zucker rat.

A growing body of literature suggests that aPKCζ/λ is a key component of the distal portions of the insulin signaling cascade, and that it is required for insulin-stimulated GLUT4 translocation (2, 3, 19, 20, 21, 24, 37, 42, 48). Previous investigations have found defective aPKCζ/λ activation in muscles of Type II diabetic rats (8, 34, 49), obese diabetic ob/ob and db/db mice (26, 50) and in cultured myotubes of obese humans (34). In addition to these studies, we have previously found that insulin-stimulated aPKCζ/λ activity is reduced in the skeletal muscle of high-fat fed rats (24, 38, 59). In the present investigation we found a significant reduction in plasma membrane aPKCζ/λ protein concentration in the obese Zucker rat, although there was no difference in cytosolic aPKCζ/λ protein concentration, under basal conditions. We also found that insulin-stimulated cytosolic and plasma membrane aPKCζ/λ protein concentration was decreased in the obese Zucker rat compared to lean littermates. In addition, we found alterations in aPKCζ/λ compartmentalization to the plasma membrane in the obese Zucker rat. Finally, there was a reduction in insulin-stimulated cytosolic and plasma

membrane aPKCζ/λ activity in the obese Zucker rat. We are unaware of any investigations that have evaluated aPKCζ/λ protein concentration and activity in the obese Zucker rat, thus our observations appear to be novel. However, these findings have also been observed in the high-fat fed rat (23, 24, 29, 38, 51, 59) as we have reported reductions in insulin-stimulated PI3-K activity, insulin-stimulated plasma membrane aPKCζ/λ protein concentration and insulin-stimulated cytosolic and plasma membrane aPKCζ/λ activities. Taken collectively these findings suggest that the insulin resistance observed in divergent models is a result of key defects in the insulin signaling cascade. Furthermore, the findings suggest that the defects are not unique to one model of insulin resistance, but that there is an underlying impairment in all models that exhibit insulin resistance.

The alterations in insulin-stimulated aPKCζ/λ protein compartmentalization and activity observed in the obese Zucker rat are likely significant as insulin-stimulated plasma membrane-associated aPKCζ/λ is believed to play a critical role in the trafficking of the GLUT4 containing vesicles to the plasma membrane. aPKCζ/λ is targeted to the plasma membrane by TC10 via its association with the Par6-Par3 complex (28, 32, 41, 43). TC10 is a component of the novel CAP/c-Cbl insulin signaling cascade and has been observed to remodel cortical actin for the trafficking of GLUT4 to the plasma membrane (6, 15, 56). Of particular note, components of the classical insulin signaling cascade (i.e. aPKCζ/λ) and the novel CAP/c-Cbl insulin signaling cascade (i.e. TC10) may work in concert to facilitate insulin-stimulated GLUT4 translocation to the plasma membrane (45). Furthermore, we (10) have recently reported that the obese Zucker rat exhibits a reduced insulin-stimulated TC10 protein concentration when compared to its lean

littermates. Taken collectively, these findings suggest that decreased insulin-stimulated plasma membrane GLUT4 protein concentration may result from a reduction in insulin-stimulated plasma membrane aPKCζ/λ protein concentration and activity and a reduction in TC10 protein concentration, further decreasing the interaction between aPKCζ/λ and TC10, thereby reducing GLUT4 trafficking.

The mechanisms behind the reduction in aPKCζ/λ protein concentration and activity in the obese Zucker rat are largely unknown. However, we have recently found possible contributors to the decrease in insulin-stimulated aPKCζ/λ activity in these animals. We have found that co-localization of a proinflammatory cytokine, SOCS-3, is increased with both IR-β and IRS-1 in the skeletal muscle of the obese Zucker rats, and that this likely resulted in why the interaction between IR-β and IRS-1 was decreased and accounts for the reduced insulin-stimulated PI3-K activity in the skeletal muscle of the obese Zucker rat (39). In addition, IKKβ serine phosphorylation was also increased in the skeletal muscle of the obese Zucker rat (39), which signifies an increased activation of IKKβ. Activated IKKβ phosphorylates IRS-1 on serine residues (22) and serine phosphorylation of IRS-1 has been linked to decreased PI3-K activity and inhibition of the distal components of the insulin signaling cascade (25, 33, 53, 61). Therefore, the reduction in insulin-stimulated PI3-K activity appears to be due to the combined effects of both SOCS-3 and IKKβ, and the reduction in insulin-stimulated PI3-K activity likely resulted in the reduced plasma membrane aPKCζ/λ concentration and activity observed in the present investigation.

Summary

In this investigation we show that plasma membrane aPKCζ/λ protein concentration is reduced in the obese Zucker rat under basal and insulin-stimulated conditions. We also show that insulin-stimulated translocation of aPKCζ/λ to the plasma membrane is reduced in the obese Zucker rat. Finally, we show that plasma membrane and cytosolic aPKCζ/λ activity is reduced in the skeletal muscle of the obese Zucker rat. It is of interest to note that alterations in insulin-stimulated aPKCζ/λ protein compartmentalization and activity found in the obese Zucker rat parallel those that we have previously observed in the high-fat fed rat (24, 38, 59). Therefore, it may be plausible that alterations in insulin-stimulated aPKCζ/λ compartmentalization and activity are not unique to any particular model of insulin resistance but instead that this may be a universal defect that is common to skeletal muscle insulin resistance regardless of its etiology.

REVIEW OF LITERATURE

Introduction

Glucose is a simple sugar sometimes referred to as blood sugar or corn sugar and is a major source of energy for our bodies. Our bodies produce glucose in the liver; however, the food we consume also serves as a source of glucose. The digestive system breaks food down into glucose, which is then delivered to cells through the bloodstream. As blood glucose levels rise pancreatic beta cells produce and release insulin, the hormone utilized to stimulate the transport of glucose from the blood into cells. In healthy individuals insulin successfully mediates the transport of glucose into the cell; however in individuals suffering from insulin resistance and diabetes, glucose transport is impaired.

Insulin resistance is a condition that occurs when the body does not properly utilize the insulin produced in the pancreas. As a result, increasing amounts of insulin are needed to regulate glucose transport into the cells and the pancreas begins to produces more insulin to compensate for the impairment in insulin function. Unfortunately, the pancreas is eventually exhausted, levels of blood glucose continue to rise in the bloodstream and our bodies become resistant to the effects of insulin thus setting the stage for diabetes (47).

Diabetes is a disease characterized by high levels of blood glucose resulting from defective insulin action, insulin production, or both. There are two major types of diabetes: type 1 diabetes and type 2 diabetes. Type 1 diabetes, also called insulin-dependent diabetes mellitus (IDDM) or juvenile-onset diabetes results when the body's immune system destroys the pancreatic beta cells that produce insulin. Approximately 5-

10% of diagnosed cases are type 1 diabetes. Type 2 diabetes also known as non-insulin-dependent diabetes mellitus (NIDDM) or adult onset diabetes accounts for about 90-95% of all diagnosed cases, usually begins as insulin resistance and is associated with older age, obesity, physical inactivity, family medical history, and race/ethnicity (23).

Diabetes was the seventh leading cause of death in the United States in 2006. As of 2007, 23.6 million people in the United States suffer from diabetes. In that year alone, 1.6 million new cases were diagnosed in people age 20 years or older. In addition, complications associated with diabetes are also on the rise including: heart disease, strokes, high blood pressure, kidney disease, nervous system disease, amputations, dental disease and complications during pregnancy (23). In 2006, the direct and indirect costs of diabetes added up to an astonishing 174 billion dollars.

Taking into consideration the amount of money that is spent treating diabetics and complications related to diabetes it is not surprising that much money has gone into research associated with diabetes and insulin resistance. Below is a review of literature related to obesity and insulin resistance, as the latter is a presumed precursor to diabetes. All aspects of this condition including glucose transport, the insulin signaling cascade and alterations in both have been reviewed. In addition, two rodent models widely used to study insulin resistance and obesity, the high-fat fed rat and the genetically obese Zucker rat, are extensively surveyed.

Glucose Transport

Insulin controls glucose levels in the blood by suppressing the production of glucose in the liver and by stimulating glucose transport into muscle and adipocytes. The transport of glucose from the blood into skeletal muscle and adipocytes is mediated by

the GLUT family of facilitative glucose transporters (62). To date, there are thirteen members of the family, GLUT1-12 and the myo-inositol transporter HMIT1. Of these family members GLUT1-4, the class I glucose transporters, are the best characterized. GLUT1 is widely expressed in tissue and is involved in glucose uptake under basal conditions. GLUT2 is expressed in beta cells and in the liver and is thought to be part of the glucose sensor. GLUT3 has a high affinity for glucose and is expressed in neurons and during fetal development. Finally GLUT4 expression is restricted to fat and muscle and is involved in insulin-stimulated glucose uptake (29, 62).

Under basal conditions, GLUT4 repeatedly recycles to and from the plasma membrane and intracellular storage vesicles. In the basal state approximately 5% of the total GLUT4 protein is continuously localized to the plasma membrane while approximately 90% of GLUT4 remains situated in intracellular storage vesicles (32) that contain proteins such as insulin-responsive aminopeptidases, synaptobrevins (v-SNARES) and Rab-4 (48, 56, 62). In response to insulin approximately 50% of GLUT4 storage vesicles move to the plasma membrane where R-SNARE VAMP2 (synaptobrevin 2) makes contact with plasma membrane localized Q_a SNARE syntaxin 4 and Q_{bc} SNARE SNAP-23 thus forming a four helix complex that is a necessary step before the vesicle fuses to the plasma membrane. Following this step other molecules including Munc18c, tomosyn and synip are thought to regulate the fusion process of GLUT4 to the plasma membrane (60). The increasing number of GLUT4 molecules at the plasma membrane increases the rate of glucose transport into the cell. Upon insulin removal, GLUT4 is internalized by the budding of clathrin-coated vesicles from the plasma

membrane and co-localizes with the early endosome marker EEA1 and the transferrin receptor where it is distributed back to intracellular vesicles (32).

Insulin Signaling

Signal transduction pathways are utilized in cells as a means to carry a signal from one cell compartment to another. Many cellular processes are made possible by these pathways including insulin signaling. Insulin signaling is the intracellular pathway used to dispose of blood glucose by causing the translocation of glucose transporters from intracellular compartments to the cell membrane. Once fused with the membrane; glucose transporters uptake glucose into skeletal muscle and/ or adipocytes where it is stored intracellularly. Presently there are two insulin signaling pathways that allow for the translocation of glucose transporters; a classical and novel cascade. The classical insulin signaling cascade begins when the insulin molecule binds to its receptor causing the activation of PI3-K and resulting in the translocation of glucose transporters to the plasma membrane. Because the translocation of glucose transporters is dependent on PI3-K, this cascade is also known as the PI3-K-dependent pathway. The novel insulin signaling cascade, which will not be discussed in detail, is believed to be involved in the docking and/or fusing of glucose transporters to the plasma membrane (11, 61).

Classical Insulin Signaling Cascade

The insulin receptor (IR) is a heterotetrameric transmembrane glycoprotein composed of two α and two β subunits, IRα and IRβ. The IRα subunits are extracellular ligand binding domains that control the kinase activity of the IRβ subunits which are composed of an extracellular domain, a membrane spanning domain and an intracellular tail (24, 44, 58, 63, 65). The IR is activated when insulin binds to the α subunits resulting

in the transautophosporylation of the IRβ subunits on three tyrosine residue sites including the juxtamembrane region. The phosphorylated IRβ subunits then interact with a family of downstream proteins; the insulin receptor substrates (IRS). To date four members of the IRS family have been identified, IRS1-4. Two of these isoforms, IRS-1 and IRS-2, are widely distributed in human and mice with IRS-1 being the most dominantly expressed in skeletal muscle (63). All IRS family members share a N-terminal pleckstrin homology (PH) and a phosphotryrosine-binding (PTB) domain. The PTB domain binds to the juxtamembrane region of the IRβ subunits at an NPEY motif (32, 48) resulting in the phosphorylation of IRS-1 at multiple sites and its subsequent activation. The phoshorylated sites on IRS-1 provide docking sites for proteins that contain Src Homology 2 (SH2) domains. Type IA phosphatidylinositol 3' kinase (PI3-K) exists in the cytosol as a heterodimer composed of a covalently associated regulatory p85 subunit and a catalytic p110 subunit. The p85 regulatory subunit contains two SH2 domains whose major role is to facilitate tyrosine kinase-dependent regulation of PI3-K activity by increasing the catalytic activity of p110. The SH2 domains of p85 have high specificity for binding phosphorylated YxxM sequences, especially YMxM motifs. IRS-1 contains YMxM motifs that once phosphorylated occupy the SH2 domains of the p85 subunit (3, 48). The binding of IRS-1 to the p85 subunit activates the catalytic p110 subunit. Once activated it dissociates from p85 and is recruited to the plasma membrane where it catalyzes the formation of PI(3, 4, 5)-trisphosphate (PIP_3) from PI(4, 5) bisphosphate (PIP_2), PIP_3 being the major product of PI3-K (63). The rise of PIP_3 levels at the plasma membrane results in the recruitment and activation of proteins that contain pleckstrin homology domains, such as 3' phosphoinositide-dependent kinase-1 and 2

(PDK-1/2). Activated PDK1/2 then phosphorylates and activates downstream proteins Akt/protein kinase B (PKB) on threonine 308 and atypical protein kinase zeta and lambda (aPKCζ/λ) on threonine 410. It is important to note that the activation of Akt/PKB and aPKCζ/λ are parallel events that stem off from PI3-K and PDK-1 and therefore do not depend on each others' functionality (52). Finally Akt/PKB and aPKCζ/λ promote the translocation of GLUT4 to the plasma membrane where it docks and fuses to the plasma membrane to uptake glucose.

Atypical protein kinase C zeta and lambda (aPKCζ/λ)

Atypical PKCζ/λ is part of the protein kinase C (PKC) family of proteins. This family is involved in many cellular functions throughout the animal and plant kingdoms. Presently there are ten PKC isotypes which are separated into three distinct groups: the classical, novel and atypical PKCs. The atypical PKC group consists of the zeta (ζ) and lambda (λ) isotypes. This group differs from the two other groups because unlike the classical and novel PKCs the aPKCs are insensitive to both calcium (Ca^{2+}) and diacylglycerol (DAG) (46) and are instead activated by phosphatidic acids and PIP_3 (43). Atypical PKCζ/λ consists of four functional domains and motifs including a PB1 domain, a pseudosubstrate (PS) sequence, a C1 domain with a single zinc finger in the N-terminus, and a kinase domain in the C-terminus. The kinase region of aPKCζ/λ contains an ATP-binding region, and activation loop, a turn motif, and a hydrophobic motif. The PS sequence blocks the substrate binding cavity of the kinase domain in what is thought of as an autoinhibition mechanism. Threonine residues 410 and 560, located in the activation loop and turn motif, respectively, are two important phosphorylation sites on

aPKCζ/λ. In addition, the protein has a phospholipid binding domain that interacts with the plasma membrane (43, 62).

The atypical PKCs exist in a folded state in which a pseudosubstrate sequence aligns with the substrate binding site and inhibits the phosphorylation of extrinsic substrates and of specific threonine residues utilized as auto and/or transphosphorylation sites by the aPKCs themselves. Acidic lipids such as PIP_3 bind to regulatory regions on aPKCζ/λ resulting in molecular unfolding and in the increase of enzymatic activity through the exposure of threonine residues, specifically threonines 410 and 411. In addition, binding of acidic lipids also increases auto and/or transphosphorylation of other threonine residues within aPKCζ/λ catalytic domains and facilitates the allosteric relief of pseudosubstrate-dependent autoinhibition (26).

Insulin activates aPKCζ/λ via phosphorylation of aPKCζ/λ by PDK-1 in the insulin signaling cascade (18, 42). PDK-1 phosphorylates the atypical PKCs on Thr 410 which lies on the T-loop of the kinase domain and also on Glu 579; an acidic residue located in the hydrophobic motif. During this process the hydrophobic motifs of aPKCζ/λ also serve as docking sites for PDK-1 (4). After this process, PIP_3 increases the autophosphorylation of Thr 560 which causes a conformational alteration resulting in the release of pseudosubstrate autoinhibition. Both the increase in autophosphorylation and PDK-1 dependent phosphorylation are required for complete activation of aPKCζ/λ (51).

A growing body of research suggests that aPKCζ/λ is an integral part of the insulin signaling cascade and its requirement for insulin-stimulated GLUT4 translocation is widely accepted (5, 8, 25, 26, 28, 30, 40, 43, 52). In support of this notion, studies which have used aPKCζ/λ inhibitors have found that insulin-stimulated glucose transport

is hindered in rat adipocytes, mouse-derived 3T3-L1 adipocytes, rat skeletal muscle preparations and rat-derived L6 myotubes (2, 6, 8, 9). Expression of kinase –inactive or activation –resistant aPKCs in the aforementioned cell lines has also resulted in inhibition of GLUT4 translocation and glucose transport (27). In addition, insulin effects on glucose transport have been hampered in mouse embryonic cell lines in which both alleles that encode aPKCζ/λ have been knocked out. Interestingly, adenoviral-mediated expression of aPKCζ/λ in these cells has completely alleviated all deleterious effects (7).

Research suggests there is defective aPKCζ/λ activation in muscles of Type II diabetic rats, monkeys and humans (13, 33, 34, 37, 38, 53, 59). Interestingly, the same defects have been found in muscles of obese diabetic ob/ob and db/db mice (31, 55), obese prediabetic mice (53), obese glucose intolerant humans (13, 59) and obese glucose tolerant humans (12, 37). In addition, insulin-stimulated aPKCζ/λ activity is decreased in cultured myotubes of obese humans and in muscle of obese diabetic monkeys (38). From this research one can also surmise that defects in aPKCζ/λ activation are seen in obesity even in the absence of diabetes; an assumption that was tested in skeletal muscle of humans with obesity and type 2 diabetes (38). Kim et al. were the first to demonstrate that in vivo insulin administration in humans activates aPKCζ/λ in skeletal muscle. In addition, they found that aPKCζ/λ protein levels were normal and that activation of aPKCζ/λ was reduced in these subjects. The conclusions of the studies mentioned above all point to impairments in the activation of IRS-1 dependent PI3-K and poor responsiveness of aPKCζ/λ to PIP_3 as the cause for defective activation of aPKCζ/λ.

Atypical PKCζ/λ activity has also been measured in high-fat fed rats. The high-fat fed rat is a rodent model that has been repeatedly used to study insulin resistance and

impairments of the insulin signaling cascade (30, 34, 41, 50, 57, 64, 66). In this model the rodents become insulin resistant by consuming a diet that is high in fat where approximately forty percent of caloric intake is derived from fat. Research has found that insulin-stimulated glucose uptake is impaired in skeletal muscle from these animals (30, 34, 57, 64). Work by Yaspelkis et al. showed a reduction in GLUT4 protein concentration and cytosolic insulin-stimulated aPKCζ/λ activity although aPKCζ/λ protein concentration was unchanged (64). In accordance with the above data, defective insulin-stimulated GLUT4 translocation was associated with reduced aPKCζ/λ activity in skeletal muscle of high-fat fed rats (34, 57). Finally, another study found that insulin-stimulated total and plasma membrane-associated aPKCζ/λ activity was reduced in muscle of high-fat fed animals (30).

The Zucker "fatty" rat

The Zucker "fatty" rat is a genetically obese rodent model used in studies on genetic obesity. The "fatty" rat resulted from a spontaneous mutation in the rat stock at the Laboratory of Comparative Pathology in Stow, Massachusetts in 1960. The condition associated with the mutation is due to a single recessive gene, *fa/fa*. The obese condition is first noted at three weeks of age and is characterized by increased body fat content, hyperinsulinism, hyperlipidemia, insulin resistance and glucose intolerance (15, 39, 68, 69). Adult Zuckers are sixty to one hundred percent overweight, compared to lean littermates, with vast subcutaneous and retroperitoneal fat deposits (67, 70). Fatty rats eat more food than lean rats and appear to be more efficient at depositing dietary energy as fat stores. In addition, the rate of *de novo* lipogenesis and the synthesis of fatty acids from glucose are increased in the fatty rat (45). In muscle and bone research, the obese rat

deposits amino acid carbon skeletons as fat instead of as muscle protein and as a result muscle development is impaired (22, 45).

The Zucker rat has been extensively studied as a model for genetic obesity (1, 10, 14, 16, 17, 19, 20, 21, 35, 49). Incidentally, research has found that insulin resistance in the Zucker rat is associated with physiological abnormalities in glucose uptake including alterations in insulin binding, reduced insulin receptor number, glucose metabolism and glucose transport (19, 20, 39). Of these defects, alterations in glucose transport seem to be the main cause of insulin resistance in the Zucker rat (16, 17, 39). In agreement, it has been reported that Zucker rat skeletal muscle glucose uptake is decreased in response to maximal insulin stimulation when measured by 3-O-methylglucose transport in hindlimb (49).

Although it is well understood that skeletal muscle glucose uptake is defective in Zucker rats, the point where the defect lies has not been clearly identified. Christ et al (19) conducted research on the skeletal muscle of the genetically obese Zucker model and found alterations in components of the insulin signaling cascade including: reductions in insulin-stimulated IRβ subunit phosphorylation, IRS-1 phosphorylation, association of p85 with IRS-1 and Akt phosphorylation. Most importantly the study found that both IRS-1 tyrosine phosphorylation and PI3-K activity are decreased in skeletal muscle of the Zucker rat, alterations that are also found in the high-fat fed rodent model. To conclude their findings, Christ et al. suggested that insulin resistance in Zucker rats is associated with decreased insulin-stimulated GLUT4 translocation to the plasma membrane. In addition, two studies conducted by Brozinick et al. (16, 17) suggest that the insulin resistance in Zucker skeletal muscle is due to a reduction in insulin-stimulated plasma

membrane GLUT4 protein concentration and activation resulting from an impairment in the translocation of GLUT4 to the plasma membrane, findings that are in agreement with Christ et al. Finally, although much work has been done on proximal components of the insulin signaling cascade in Zucker skeletal muscle, research has largely overlooked the role that aPKCζ/λ plays in insulin signaling in the Zucker rat, even though it has been proven to be required for insulin-stimulated glucose uptake (8, 26, 41, 44, 53).

Summary

In summary, diabetes is a disease developed as a result of genetic or environmental factors, specifically a poor diet and a sedentary lifestyle. The costs associated with diabetes and diabetes-related conditions add up to millions of dollars a year in medical expenses. Research conducted in efforts to better understand the disease has found that the condition is associated with impairments in glucose uptake and transport resulting from alterations in components of the insulin signaling cascade. Various environmental and genetic insulin resistant animal models have been used to study whether elements associated to the disease differ in the models and to find possible similarities in the mechanism of impairment in the animal models. Collectively, the results obtained from these investigations have enhanced the current body of knowledge and have helped to begin elucidating the many questions surrounding the origins and effects of the disease.

REFERENCES

For Abstract, Introduction, Methods, Results & Discussion

1. Anai M, Funaki M, Ogihara T, Terasaki J, Inukai K, Katagiri H, Fukushima Y, Yazaki Y, Kikuchi M, Oka Y, and Asano T. Altered expression levels and impaired steps in the pathway to phosphatidylinositol 3-kinase activation via insulin receptor substrates 1 and 2 in Zucker fatty rats. *Diabetes* 47: 13-23, 1998

2. Bandyopadhyay G, Kanoh Y, Sajan MP, Standaert ML, and Farese RV. Effects of adenoviral gene transfer of wild-type, constitutively active, and kinase-defective protein kinase C-λ on insulin-stimulated glucose transport in L6 myotubes. *Endocrinology* 141: 4120-4127, 1999

3. Bandyopadhyay G, Standaert ML, Sajan MP, Kanoh Y, Miura A, Braun U, Kruse F, Leitges M, and Farese RV. Protein kinase C-λ knockout in embryonic stem cells and adipocytes impairs insulin-stimulated glucose transport. *Mol Endocrinol* 18: 373-383, 2004

4. Bandyopadhyay G, Standaert ML, Sajan MP, Karnitz LM, Cong L, Quon MJ, and Farese RV. Dependence of Insulin-Stimulated Glucose Transporter 4 Translocation on 3-Phophoinositide-Dependent Protein Kinase-1 and Its Target Threonine-410 in the Activation Loop of Protein Kinase C-ζ. *Mol Endocrinol* 13: 1766-1772, 1999

5. Banks EA, Brozinick JT Jr, Yaspelkis BB 3rd, Kang HY, and Ivy JL. Muscle glucose transport, GLUT-4 content, and degree of exercise training in obese Zucker rats. *Am J Physiol* 263: E1010-E1015, 1992

6. Baumann CA, Ribon V, Kanzaki M, Thurmond DC, Mora S, Shigematsu, Bickel PE, Pessin JE, and Saltiel AR. CAP defines a second signalling pathway required for insulin-stimulated glucose transport. *Nature* 407: 202-207, 2000

7. Beeson M, Sajan MP, Daspet JG, Luna V, Dizon M, Grebenev D, Powe JL, Lucidi S, Miura A, Kanoh Y, Bandyopadhyay G, Standaert ML, Yeko TR, and Farese RV. Defective activation of Protein Kinase C-z in Muscle by Insulin and Phosphatidylinositol-3,4,5,-(PO(4))(3) in Obesity and Polycystic Ovary Syndrome. *Metab Syndr Relat Dis* 2: 49-56, 2004

8. Beeson M, Sajan MP, Dizon M, Grebenev D, Daspet GJ, Miura A, Kanoh Y, Powe J, Banyopadhyay G, Standaert ML, and Farese RV. Activation of Protein Kinase C-ζ by Insulin and Phophatidylinositol-3, 4, 5-$(PO_4)_3$ Is Defective in Muscle in Type 2 Diabetes and Impaired Glucose Tolerance. *Diabetes* 52: 1926-1935, 2003

9. Bernard JR, Reeder DW, Herr HJ, Rivas DA, and Yaspelkis BB, III. High-fat feeding effects on components of the CAP/Cbl signaling cascade in Sprague-Dawley rat skeletal muscle. *Metabolism* 55: 203-212, 2006

10. Bernard JR, Saito M, Liao YH, Yapspelkis BB, III, and Ivy JL. Exercise training increases components of the c-Cbl-associated protein/c-Cbl signaling cascade in muscle of obese Zucker rats. *Metabolism* 57: 858-866, 2008

11. Bradford MM. A rapid and sensitive method for the quantitation of microgram quantities of protein utilizing the principle of protetin-dye binding. *Anal Biochem* 72: 248-254, 1976

12. Brozinick JT Jr, Etgen GJ Jr, Yaspelkis BB, III, and Ivy JL. Glucose uptake and GLUT-4 protein distribution in skeletal muscle of the obese Zucker rat. *Am J Physiol* 267: R234-R243, 1994

13. Brozinick JT Jr, Etgen GJ Jr, Yaspelkis BB, III, Kang HY, and Ivy JL. Effects of exercise training on muscle GLUT-4 protein content and translocation in obese Zucker rats. *Am J Physiol Endocrinol Metab* 265: E419-E427, 1993

14. Carvalho E, Rondinone C, and Smith U. Insulin resistance in fat cells from obese Zucker rats-Evidence for an impaired activation and translocation of protein kinase B and glucose transporter 4. *Mol Cell Biochem* 206: 7-16, 2000

15. Chiang SH, Baumann CA, Kanzaki M, Thurmond DC, Watson RT, Neudauer CL, Macara IG, Pessin JE, and Saltiel AR. Insulin-stimulated GLUT4 translocation requires the CAP-dependent activation of TC10. *Nature* 410: 944-948, 2001

16. Christ CY, Hunt D, Hancock J, Garcia-Macedo R, Mandarino LJ, and Ivy JL. Exercise training improves muscle insulin resistance but not insulin receptor signaling in obese Zucker rats. *J Appl Physiol* 92: 736-744, 2002

17. Crettaz M, Prentki M, Zaninetti D, and Jeanrenaud B. Insulin resistance in soleus muscle from obese Zucker rats: involvement of several defective sites. *Biochem J* 186: 525-534, 1980

18. Czech MP, Richardson DK, Becker SG, Walters CG, Gitomer W, and Heinrich J. Insulin response in skeletal muscle and fat cells of the genetically obese Zucker rat. *Metab Clin Exp* 27: 1967-1981, 1978

19. Etgen GJ, Valasek KM, Broderick CL, and Miller AR. *In Vivo* Adenoviral Delivery of Recombinant Human Protein Kinase C-ζ Stimulates Glucose Transport Activity in Rat Skeletal Muscle. *J Biol Chem* 274: 22139-22142, 1999

20. Farese RV. Function and dysfunction of aPKC isoforms for glucose transport in insulin-sensitive and insulin-resistant states. *Am J Physiol Endocrinol Metab* 283: E1-E11, 2002

21. Farese RV, Sajan MP, and Standaert ML. Insulin-Sensitive Protein Kinases (Atypical Protein Kinase C and Protein Kinase B/Akt): Actions and Defects in Obesity and Type II Diabetes. *Exp Biol (Maywood)* 230: 593-605, 2005

22. Gao Z, Hwang D, Bataille F, Lefevre M, York D, Quon MJ, and Ye J. Serine phosphorylation of insulin receptor substrate 1 by inhibitor κB kinase complex. *J Biol Chem* 277: 48115-48121, 2002

23. Hansen PA, Han DH, Marshall BA, Nolte LA, Chen MM, Mueckler M, and Holloszy JO. A high fat diet impairs stimulation of glucose transport in muscle. Functional evaluation of potential mechanisms. *J Biol Chem* 273: 26157-26163, 1998

24. Herr HJ, Bernard JR, Reeder DW, Rivas DA, Limon JJ, and Yaspelkis BB, III. Insulin-stimulated plasma membrane association and activation of Akt2, aPKCζ and aPKCλ in high fat fed rodent skeletal muscle. *J Physiol* 565: 627-636, 2005

25. Hirosumi J, Tuncman G, Chang LF, Gorgun CZ, Uysal KT, maedda K, Karin M, and Hotamisligil GS. A central role for JNK in obesity and insulin resistance. *Nature* 420: 333-336, 2005

26. Hori H, Sasaoka T, Ishihara H, Wada T, Murakami MS, Ishiki M, and Kobayashi M. Association of SH2-containing inositol phosphatase 2 with the insulin resistance of diabetic db/db mice. *Diabetes* 51: 2387-2394, 2002

27. Ivy JL, Brozinick JT, Jr., Torgan CE, and Kastello GM. Skeletal muscle glucose transport in obese Zucker rats after exercise training. J Appl Physiol 66: 2635-3641, 1989

28. Joberty G, Petersen C, Gao L, and Macara IG. The cell-polarity protein Par6 links Par3 and atypical protein kinase C to Cdc42. *Nat Cell Biol* 2: 531-539, 2000

29. Kanoh Y, Bandyopadhyay G, Sajan MP, Standaert ML, and Farese RV. Rosiglitazone, insulin treatment, and fasting correct defective activation of protein kinase C-zeta/lambda by insulin in vastus lateralis muscles and adipocytes of diabetic rats. *Endocrinology* 142: 1595-1605, 2001

30. Kanoh Y, Sajan MP, Bandyopadhyay G, Miura A, Standaert ML, and Farese RV. Defective Activation of Atypical Protein Kinase C ζ and λ by Insulin and Phosphatidylinositol-3, 4, 5-$(PO_4)_3$ in Skeletal Muscle of Rats Following High-Fat Feeding and Streptozotocin-Induced Diabetes. *Endocrinology* 144: 947-954, 2003

31. Kanzaki M, Mora S, Hwang JB, Saltiel AR, and Pessin JE. Atypical protein kinase C (aPKC z/l) is a convergent downstream target of the insulin-stimulated phosphatidylinositol 3-kinase and TC10 signaling pathways. *J Cell Biol* 164: 279-290, 2004

32. Kemmer FW, Berger M, Herberg L, Gries FA, Wirdeier A, and Becker K. Glucose metabolism in perfused skeletal muscle: demonstration of insulin resistance in obese Zucker rat. *Biochem J* 178: 733-741, 1979

33. Kim JK, Fillmore JJ, Sunshine MJ, Albrecht B, Higashimori T, Kim DW, Liu ZX, Soos TJ, Cline GW, O'Brien WR, Littman DR, and Shulman GI. PKC-τ knockout mice are protected from fat-induced insulin resistance. *J Clin Invest* 114: 823-827, 2004

34. Kim YB, Kotani K, Ciaraldi TP, Henry RR, and Kahn BB. Insulin-Stimulated Protein Kinase C λ/ζ Activity Is Reduced in Skeletal Muscle of Humans with Obesity and Type 2 Diabetes. *Diabetes* 52: 1935-1942, 2003

35. Kim YB, Nikoulina SE, Ciaraldi TP, Henry RR, and Kahn BB. Normal insulin-dependent activation of Akt/protein kinase B, with diminished activation of phosphoinositide 3-kinase, in muscle in type 2 diabetes. *J Clin Invest* 104: 733-741, 1999

36. King PA, Horton ED, Hirshman MF, and Horton ES. Insulin Resistance in Obese Zucker Rat (fa/fa) Skeletal Muscle Is Associated with a Failure of Glucose Transporter Translocation. *J Clin Invest* 90: 1568-1575, 1992

37. Kotani K, Ogawa W, Matsumoto M, Kitamura T, Sakaue H, Hino Y, Miyake K, Wataru S, Akimoto K, Ohno S, and Kasuga M. Requirement of Atypical Protein Kinase Cλ for Insulin Stimulation of Glucose Uptake but Not for Akt Activation in 3T3-L1 Adipocytes. *Mol Cell Biol* 18: 6971-6982, 1998

38. Krisan AD, Colling DE, Crain AM, Kwong CC, Singh MD, Bernard JR, and Yaspelkis BB, III. Resistance training enhances components of the insulin signaling cascade in normal and high-fat-fed rodent skeletal muscle. *J Appl Physiol* 96: 1691-1700, 2004

39. Kvasha IA. (2009) *Activation of Inflammatory pathways impairs insulin signaling in obese Zucker rat skeletal muscle.* Masters thesis. California State University Northridge

40. Lessard SJ, LoGiudice SL, Lau W, Reid J, Turner N, Febbraio MF, Hawley JA, and Watt MJ. Rosiglitazone enhances glucose tolerance by mechanisms other than reduction of fatty acid in skeletal muscle. *Endocrinol* 145: 5665-5670, 2004

41. Lin D, Edwards AS, Fawcett JP, Mbamalu G, Scott JD, and Pawson T. A mammalian PAR-3-PAR-6 complex implicated in Cdc42/Rac1 and aPKC signaling and cell polarity. *Nat Cell Biol* 2: 540-547, 2000

42. Liu LZ, He AB, Liu XJ, Li Y, Chang YS, and Fang FD. Protein Kinase Cζ and Glucose Uptake. *Biochemistry (Mosc)* 71: 701-706, 2006

43. Noda Y, Takeya R, Ohno S, Naito S, Ito T, and Sumimoto H. Human homologues of the *Caenorhabditis elegans* cell polarity protein PAR6 as an adaptor that links the small GTPases Rac and Cdc42 to atypical protein kinase C. *Genes Cells* 6: 107-119, 2001

44. Ruderman NB, Houghton CRS, and Helms R. Evaluation of the isolated perfused rat hindquarter for the study of muscle metabolism. *Biochem J* 124: 639-651, 1971

45. Saito M, Lessard SJ, Rivas DA, Redder DW, Hawley JA, and Yaspelkis BB, III. Activation of atypical protein kinase Czeta toward TC10 is regulated by high-fat diet and aerobic exercise in skeletal muscle. *Metabol* 57: 1173-1180, 2008

46. Sherman WM, Katz AL, Cutler CL, Withers RT, and Ivy JL. Glucose transport: locus of muscle insulin resistance in obese Zucker rats. *Am J Physiol Endocrinol Metab* 255: E374-E382, 1988

47. Singh MK, Krisan AD, Crain AM, Collins DE, and Yapselkis BB, III. High-fat diet and leptin treatment alter skeletal muscle insulin-stimulated phophotidylinositol 3-kinase activity and glucose transport. *Metabol* 52: 1196-1205, 2003

48. Standaert ML, Bandyopadhyay G, Perez L, Price D, Galloway L, Poklepovic A, Sajan MP, Cenni V, Sirri A, Moscat J, Toker A, and Farese RV. Insulin activates Protein Kinases C-ζ and C-λ by and autophosphorylation-dependent mechanism and stimulates their translocation to GLUT4 vesicles and other membrane fractions in rat adipocytes. *J Biol Chem* 274: 25308-25316, 1999

49. Standaert ML, Ortmeyer HK, Hansen BC, Sajan MP, Kanoh Y, Bandyopadhyay G, and Farese RV. Skeletal muscle insulin resistance in obesity-associated type 2 diabetes in monkeys is linked to a defect in insulin activation of protein kinase C-zeta/lambda/iota. *Diabetes* 51: 2936-2943, 2002

50. Standaert ML, Sajan MP, Miura A, Kanoh Y, Chen HC, Farese Rv Jr, and Farese RV. Insulin-induced activation of atypical protein kinase C, but not protein kinase B, is maintained in diabetic (ob/ob and Goto-Kakazaki) liver. Contrasting insulin signaling patterns in liver versus muscle define phenotypes of type 2 diabetic and high fat-induced insulin-resistant states. *J Biol Chem* 279: 24929-24934, 2004

51. Thong FSL, Dugani CB, and Klip A. Turning Signals On and Off: GLUT4 Traffic in the Insulin-Signaling Highway. *Physiology* 20: 271-284, 2005

52. Tremblay F, Lavigne C, Jacques H, and Marette A. Defective insulin-induced GLUT4 translocation in skeletal muscle of high fat fed rats is associated with alterations in both Akt/Protein Kinase B and atypical Protein Kinase C (ζ/λ) activities. *Diabetes* 50: 1901-1910, 2001

53. Um SH, Frigerio F, Watanaabe M, Picard F, Joaqui M, Sticker M, Funagalli S, Allegrini PR, Kozma SC, Auwerx J, and Thomas G. Absence of S6K1 protects against age-and diet-induced obesity while enhancing insulin sensitivity. *Nature* 431: 200-205, 2004

54. Vollenweider P, Menard B, and Nicod P. Insulin resistance, defective insulin receptor substrate 2-associated phosphatidylinositol-3' kinase activation, and impaired atypical protein kinase C (zeta/lambda) activation in myotubes from obese patients with impaired glucose tolerance. *Diabetes* 51: 1052-1059, 2002

55. Wadley GD, Bruce CR, Konstantopoulos N, Macaulay SL, Howlett KF, and Hawley JA. The effect of insulin and exercise on c-Cbl protein abundance and phosphorylation in insulin-resistant skeletal muscle in lean and obese Zucker rats. *Diabetologia* 47: 412-419, 2004

56. Watson RT, Shigematsu S, Chiang SH, Mora S, Kanzaki M, Macara IG, Saltiel AR, and Pessin JE. Lipid raft microdomain compartmentalization of TC10 is required for insulin signaling and GLUT4 translocation. *J Cell Biol* 154: 829-840, 2001

57. Yaspelkis BB, III, Davis FR, Saberi M, Smith TL, Jazayeri R, Singh M, Fernandez V, Trevino B, Chinookoswong N, Wang J, Shi ZQ, and Levin N. Leptin administration improves skeletal muscle insulin responsiveness in diet-induced insulin-resistance rats. *Am J Physiol Endocrinol Metab* 280: E130-E142, 2001

58. Yaspelkis BB, III, Kvasha IA, and Figueroa TY. High-fat feeding increases insulin receptor and IRS-1 coimmunoprecipitation with SOCS-3, IKKα/β phosphorylation and decreases PI-3 kinase activity in muscle. *Am J Physiol Regu Integr Comp Physiol* 296: R1709-R1715, 2009

59. Yaspelkis BB, III, Lessard SJ, Reeder DW, Limon JJ, Saito M, Rivas DA, Kvasha I, and Hawley JA. Exercise reverses high-fat diet-induced impairments on compartmentalization and activation of components of the insulin-signaling cascade in skeletal muscle. *Am J Physiol Endocrinol Metab* 293: E941-E949, 2007

60. Yaspelkis BB, III, Singh MK, Krisan AD, Collins DE, Kwong CC, Bernard JR, and Crain AM. Chronic leptin treatment enhances insulin-stimulated glucose disposal in skeletal muscle of high-fat fed rodents. *Life Sci* 74: 1801-1816, 2004

61. Yu CL, Chen Y, Cline GW, Zhang DY, Zong HH, Wang YL, Bergeron R, Kim JK, Cushman SW, Cooney GJ, Atcheson B, White MF, Kraegen EW, and Shulman GI. Mechanism by which fatty acids inhibit insulin activation of insulin receptor substrate-1 (IRS-1)-associated phosphatidylionositol 3-kinase activity in muscle. *J Biol Chem* 277: 50230-50236, 2002

62. Zierath JR, Houseknecht KL, Gnudi L, and Kahn BB. High-fat feeding impairs insulin-stimulated GLUT recruitment via and early insulin-signaling defect. *Diabetes* 46: 215-219, 1997

For Review of Literature

1. Anai M, Funaki M, Ogihara T, Terasaki J, Inukai K, Katagiri H, Fukushima Y, Yazaki Y, Kikuchi M, Oka Y, and Asano T. Altered expression levels and impaired steps in the pathway to phosphatidylinositol 3-kinase activation via insulin receptor substrates 1 and 2 in Zucker fatty rats. *Diabetes* 47: 13-23, 1998

2. Avignon A, Standaert ML, Yamada K, Mischak H, Spencer B, and Farese RV. Insulin increases mRNA levels of protein kinase C-α and –β in rat adipocytes and protein kinase C-α, -β and θ in rat skeletal muscle. *Biochem J* 308: 181-187, 1995

3. Backer JM, Myers MG Jr, Shoelson SE, Chin DJ, Sun XJ, Miralpeix M, Hu P, Margolis B, Skolnik EY, Schlessinger J, and White MF. Phosphatidylinositol 3'-kinase is activated by association with IRS-1 during insulin stimulation. *EMBO J* 11: 3469-3479, 1992

4. Balendran A, Biondi RM, Cheung PCF, Casamayor A, Deak M, and Alessi DR. A 3-Phosphoinositide-dependent Protein Kinase-1 (PDK10 Docking Site Is Required for the Phosphorylation of Protein Kinase Cζ (PKCζ) and PKC-related Kinase 2 by PDK1. *J Biol Chem* 275: 20806-20813, 2000

5. Bandyopadhyay G, Kanoh Y, Sajan MP, Standaert ML, and Farese RV. Effects of adenoviral gene transfer of wild-type, constitutively active, and kinase-defective protein kinase C-λ on insulin-stimulated glucose transport in L6 myotubes. *Endocrinology* 141: 4120-4127, 1999

6. Bandyopadhyay G, Standaert ML, Galloway L, Moscat J, and Farese RV. Evidence for involvement of protein kinase C (PKC)-ζ and noninvolvement of diacylglycerol-sensitive PKCs in insulin-stimulated glucose transport in L6 myotubes. *Endocrinology* 138: 4721-4731, 1997

7. Bandyopadhyay G, Standaert ML, Sajan MP, Kanoh Y, Miura A, Braun U, Kruse F, Leitges M, and Farese RV. Protein kinase C-λ knockout in embryonic stem cells and adipocytes impairs insulin-stimulated glucose transport. *Mol Endocrinol* 18: 373-383, 2004

8. Bandyopadhyay G, Standaert ML, Sajan MP, Karnitz LM, Cong L, Quon MJ, and Farese RV. Dependence of Insulin-Stimulated Glucose Transporter 4 Translocation on 3-Phophoinositide-Dependent Protein Kinase-1 and Its Target Threonine-410 in the Activation Loop of Protein Kinase C-ζ. *Mol Endocrinol* 13: 1766-1772, 1999

9. Bandyopadhyay G, Standaert ML, Zhao L, Yu B, Avignon A, Galloway L, Karnam P, Moscat J, and Farese RV. Activation of protein kinase C(α, β, and ζ) by insulin in 3T3/L1 cells. Transfection studies suggest a role for PKC-ζ in glucose transport. *J Biol Chem* 272: 2551-2558, 1997

10. Banks EA, Brozinick JT Jr, Yaspelkis BB 3rd, Kang HY, and Ivy JL. Muscle glucose transport, GLUT-4 content, and degree of exercise training in obese Zucker rats. *Am J Physiol* 263: E1010-E1015, 1992

11. Baumann CA, Ribon V, Kanzaki M, Thurmond DC, Mora S, Shigematsu , Bickel PE, Pessin JE, and Saltiel AR. CAP defines a second signaling pathway required for insulin-stimulated glucose transport. *Nature* 407: 202-207, 2000

12. Beeson M, Sajan MP, Daspet JG, Luna V, Dizon M, Grebenev D, Powe JL, Lucidi S, Miura A, Kanoh Y, Bandyopadhyay G, Standaert ML, Yeko TR, and Farese RV. Defective activation of Protein Kinase C-z in Muscle by Insulin and Phosphatidylinositol-3,4,5,-(PO(4))(3) in Obesity and Polycystic Ovary Syndrome. *Metab Syndr Relat Dis* 2: 49-56, 2004

13. Beeson M, Sajan MP, Dizon M, Grebenev D, Daspet GJ, Miura A, Kanoh Y, Powe J, Banyopadhyay G, Standaert ML, and Farese RV. Activation of Protein Kinase C-ζ by Insulin and Phophatidylinositol-3, 4, 5-$(PO_4)_3$ Is Defective in Muscle in Type 2 Diabetes and Impaired Glucose Tolerance. *Diabetes* 52: 1926-1935, 2003

14. Bernard JR, Saito M, Liao YH, Yapspelkis BB III, and Ivy JL. Exercise training increases components of the c-Cbl-associated protein/c-Cbl signaling cascade in muscle of obese Zucker rats. *Metabolism* 57: 858-866, 2008

15. Bray GA. The Zucker-fatty rat: a review. *Federation Proc* 36: 148-153, 1977

16. Brozinick JT Jr, Etgen GJ Jr, Yaspelkis BB, III, and Ivy JL. Glucose uptake and GLUT-4 protein distribution in skeletal muscle of the obese Zucker rat. *Am J Physiol* 267: R234-R243, 1994

17. Brozinick JT Jr, Etgen GJ Jr, Yaspelkis BB, III, Kang HY, and Ivy JL. Effects of exercise training on muscle GLUT-4 protein content and translocation in obese Zucker rats. *Am J Physiol Endocrinol Metab* 265: E419-E427, 1993

18. Chou MM, Hou W, Johnson J, Graham LK, Lee MH, Chen CS, Newton AC, Schaffhausen BS, and Toker A. Regulation of protein kinase C ζ by PI 3-kinase and PDK-1. *Current Biology* 8: 1069-1077, 1998

19. Christ CY, Hunt D, Hancock J, Garcia-Macedo R, Mandarino LJ, and Ivy JL. Exercise training improves muscle insulin resistance but not insulin receptor signaling in obese Zucker rats. *J Appl Physiol* 92: 736-744, 2002

20. Crettaz M, Prentki M, Zaninetti D, and Jeanrenaud B. Insulin resistance in soleus muscle from obese Zucker rats: involvement of several defective sites. *Biochem J* 186: 525-534, 1980

21. Czech MP, Richardson DK, Becker SG, Walters CG, Gitomer W, and Heinrich J. Insulin response in skeletal muscle and fat cells of the genetically obese Zucker rat. *Metab Clin Exp* 27: 1967-1981, 1978

22. Deb S, Martin RJ, and Hershberger TV. Maintenance requirement and energetic efficiency of lean and obese Zucker rats. *J Nutr* 106: 191-197, 1976

23. Department of Health and Services, Center for Disease Control and Prevention (CDC) (2007). National Diabetes Fact Sheet. Retrieved March 10, 2009, from http://www.cdc.gov/diabetes/pubs/pdf/ndfs_2007pdf

24. Ebina Y, Ellis L, Jarnagin K, Edery M, Graf L, Clauser E, Ou JH, Masiar F, Kan YW, Goldfine ID, Roth RA, and Rutter WJ. The human insulin receptor cDNA: the structural basis for hormone activated transmembrane signalling. *Cell* 40: 747-758, 1985

25. Etgen GJ, Valasek KM, Broderick CL, and Miller AR. *In Vivo* Adenoviral Delivery of Recombinant Human Protein Kinase C-ζ Stimulates Glucose Transport Activity in Rat Skeletal Muscle. *J Biol Chem* 274: 22139-22142, 1999

26. Farese RV. Function and dysfunction of aPKC isoforms for glucose transport in insulin-sensitive and insulin-resistant states. *Am J Physiol Endocrinol Metab* 283: E1-E11, 2002

27. Farese RV, Sajan MP, and Standaert ML. Atypical protein kinase C in insulin action and insulin resistance. *Biochemical Society Transactions* 33: 350-353, 2005

28. Farese RV, Sajan MP, and Standaert ML. Insulin-Sensitive Protein Kinases (Atypical Protein Kinase C and Protein Kinase B/Akt): Actions and Defects in Obesity and Type II Diabetes. *Exp Biol (Maywood)* 230: 593-605, 2005

29. Garvey WT, Maianu L, Zhu JH, Brechtel-Hook G, Wallace P, and Baron AD. Evidence for Defects in the Trafficking and Translocation of GLUT4 Glucose Transporters in Skeletal Muscle as a Cause for Human Insulin Resistance. *J Clin Invest* 101: 2377-2386, 1998

30. Hansen PA, Han DH, Marshall BA, Nolte LA, Chen MM, Mueckler M, Holloszy JO. A high fat diet impairs stimulation of glucose transport in muscle. Functional evaluation of potential mechanisms. *J Biol Chem* 273: 26157-26163, 1998

31. Herr HJ, Bernard JR, Reeder DW, Rivas DA, Limon JJ, and Yaspelkis BB, III. Insulin-stimulated plasma membrane association and activation of Akt2, aPKCζ and aPKCλ in high fat fed rodent skeletal muscle. *J Physiol* 565: 627-636, 2005

32. Hori H, Sasaoka T, Ishihara H, Wada T, Murakami MS, Ishiki M, and Kobayashi M. Association of SH2-containing inositol phosphatase 2 with the insulin resistance of diabetic db/db mice. *Diabetes* 51: 2387-2394, 2002

33. Hou JC, and Pessin JE. Ins (endocytosis) and outs (exocytosis) of GLUT4 trafficking. *Current Opinion in Cell Biology* 19: 466-473, 2007

34. Kanoh Y, Bandyopadhyay G, Sajan MP, Standaert ML, and Farese RV. Rosiglitazone, insulin treatment, and fasting correct defective activation of protein kinase C-zeta/lambda by insulin in vastus lateralis muscles and adipocytes of diabetic rats. *Endocrinology* 142: 1595-1605, 2001

35. Kanoh Y, Sajan MP, Bandyopadhyay G, Miura A, Standaert ML, and Farese RV. Defective Activation of Atypical Protein Kinase C ζ and λ by Insulin and Phosphatidylinositol-3, 4, 5-$(PO_4)_3$ in Skeletal Muscle of Rats Following High-Fat Feeding and Streptozotocin-Induced Diabetes. *Endocrinology* 144: 947-954, 2003

36. Kemmer FW, Berger M, Herberg L, Gries FA, Wirdeier A, and Becker K. Glucose metabolism in perfused skeletal muscle: demonstration of insulin resistance in obese Zucker rat. *Biochem J* 178: 733-741, 1979

37. Khan AH, and Pessin JE. Inulin regulation of glucose uptake: a complex interplay of intracellular signalling pathways. *Diabetalogia* 45: 1475-1483, 2002

38. Kim YB, Kotani K, Ciaraldi TP, Henry RR and Kahn BB. Normal insulin-dependent activation of Akt/protein kinase B, with diminished activation of phosphoinositide 3-kinase, in muscle in type 2 diabetes. *J Clin Invest* 104: 733-741, 1999

39. Kim YB, Kotani K, Ciaraldi TP, Henry RR, and Kahn BB. Insulin-Stimulated Protein Kinase C λ/ζ Activity Is Reduced in Skeletal Muscle of Humans with Obesity and Type 2 Diabetes. *Diabetes* 52: 1935-1942, 2003

40. King PA, Horton ED, Hirshman MF, and Horton ES. Insulin Resistance in Obese Zucker Rat (fa/fa) Skeletal Muscle Is Associated with a Failure of Glucose Transporter Translocation. *J Clin Invest* 90: 1568-1575, 1992

41. Kotani K, Ogawa W, Matsumoto M, Kitamura T, Sakaue H, Hino Y, Miyake K, Wataru S, Akimoto K, Ohno S, and Kasuga M. Requirement of Atypical Protein Kinase Cλ for Insulin Stimulation of Glucose Uptake but Not for Akt Activation in 3T3-L1 Adipocytes. *Mol Cell Biol* 18: 6971-6982, 1998

42. Krisan AD, Colling DE, Crain AM, Kwong CC, Singh MD, Bernard JR, and Yaspelkis BB, III. Resistance training enhances components of the insulin signaling cascade in normal and high-fat-fed rodent skeletal muscle. *J Appl Physiol* 96: 1691-1700, 2004

43. Le Good JA, Ziegler WH, Parekh DB, Alessi DR, Cohen P, and Parker PJ. Protein Kinase C Isotypes controlled by Phosphoinositide 3-Kinase through the Protein Kinase PDK1. *Science* 281: 2042-2045, 1998

44. Liu LZ, He AB, Liu XJ, Li Y, Chang YS, and Fang FD. Protein Kinase Cζ and Glucose Uptake. *Biochemistry (Mosc)* 71: 701-706, 2006

45. Martin G, Myers Jr, and Morris F. The new elements of insulin signaling: Insulin receptor substrate-1 and proteins with SH2 domains. *Diabetes* 42: 643-648, 1993

46. Martin RJ. Genetic influence on nutritional aspects of metabolic regulation. *Fed Proc* 35: 2291-2294, 1976

47. Mellor H, and Parker PJ. The extended protein kinase C superfamily. *Biochem J* 332: 281-292, 1998

48. National Diabetes Information Clearinghouse, National Institute Of Diabetes And Digestive And Kidney Diseases. Insulin Resistance and Pre-diabetes. Retrieved March 10, 2009, from http://diabetesniddk.nih.gov/DM/pubs /insulinresistance/insulinresistance .pdf

49. Shepherd RR, Withers DJ, and Siddle K. Phosphoinositide 3-kinase: the key switch mechanism in insulin signaling. *Biochem J* 333: 471-490, 1998

50. Sherman WM, Katz AL, Cutler CL, Withers RT, and Ivy JL. Glucose transport: locus of muscle insulin resistance in obese Zucker rats. *Am J Physiol Endocrinol Metab* 255: E374-E382, 1988

51. Singh MK, Krisan AD, Crain AM, Collins DE, and Yapselkis BB, III. High-fat diet and leptin treatment alter skeletal muscle insulin-stimulated phophotidylinositol 3-kinase activity and glucose transport. *Metabol* 52: 1196-1205, 2003

52. Standaert ML, Bandyopadhyay G, Kanoh Y, Sajan MP, and Farese RV. Insulin and PIP_3 activate PKC-ζ by mechanisms that are both dependent and independent of Phosphorylation of Activation Loop (T410) and Autophosphorylation (T560) Sites. *Biochemistry* 40: 249-255, 2001

53. Standaert ML, Bandyopadhyay G, Perez L, Price D, Galloway L, Poklepovic A, Sajan MP, Cenni V, Sirri A, Moscat J, Toker A, and Farese RV. Insulin activates Protein Kinases C-ζ and C-λ by and autophosphorylation-dependent mechanism and stimulates their translocation to GLUT4 vesicles and other membrane fractions in rat adipocytes. *J Biol Chem* 274: 25308-25316, 1999

54. Standaert ML, Ortmeyer HK, Hansen BC, Sajan MP, Kanoh Y, Bandyopadhyay G, and Farese RV. Skeletal muscle insulin resistance in obesity-associated type 2 diabetes in monkeys is linked to a defect in insulin activation of protein kinase C-zeta/lambda/iota. *Diabetes* 51: 2936-2943, 2002

55. Standaert ML, Sajan MP, Miura A, Bandyopadhyay G, and Farese RV. Requirements for pYXXM motifs in Cbl for binding to the p85 subunit of Phosphatidylinositol 3-Kinase and Crk, and activation of atypical Protein Kinase C and glucose transport during insulin action in 3T3/L1 adipocytes. *Biochemistry* 43: 15494-15502, 2004

56. Standaert ML, Sajan MP, Miura A, Kanoh Y, Chen HC, Farese Rv Jr, and Farese RV. Insulin-induced activation of atypical protein kinase C, but not protein kinase B, is maintained in diabetic (ob/ob and Goto-Kakazaki) liver. Contrasting insulin signaling patterns in liver versus muscle define phenotypes of type 2 diabetic and high fat-induced insulin-resistant states. *J Biol Chem* 279: 24929-24934, 2004

57. Thong FSL, Dugani CB, and Klip A. Turning Signals On and Off: GLUT4 Traffic in the Insulin-Signaling Highway. *Physiology* 20: 271-284, 2005

58. Tremblay F, Lavigne C, Jacques H, and Marette A. Defective insulin-induced GLUT4 translocation in skeletal muscle of high fat fed rats is associated with alterations in both Akt/Protein Kinase B and atypical Protein Kinase C (ζ/λ) activities. *Diabetes* 50: 1901-1910, 2001

59. Ullrich A, Bell FR, Chen EY, Herrera R, Petruzzelli LM, Dull TJ, Gray A, Coussens L, Liao YC, Tsubokawa M, Mason A, Seeburg PH, Grunfeld C, Rosen OM, and Ramachandran J. Human insulin receptor and its relationship to the tyrosine kinase family of oncogenes. *Nature* 313:756-761, 1985

60. Vollenweider P, Menard B, and Nicod P. Insulin resistance, defective insulin receptor substrate 2-associated phosphatidylinositol-3' kinase activation, and impaired atypical protein kinase C (zeta/lambda) activation in myotubes from obese patients with impaired glucose tolerance. *Diabetes* 51: 1052-1059, 2002

61. Watson RT, and Pessin JE. GLUT4 translocation: The last 200 nanometers. *Cellular Signalling* 19: 2209-2217, 2007

62. Watson RT, and Pessin JE. Subcellular compartmentalization and trafficking of the insulin-responsive glucose transporter, GLUT4. *Exp Cell Res* 271: 75-83, 2001a

63. Webb BL, Hirst SJ, and Giembycz MA. Protein kinase C isoenzymes: A review of their structure, regulation and role in regulating airways smooth muscle tone and mitogenesis. *Br J Pharmacol* 130: 1433-1452, 2000

64. White MF. IRS proteins and the common path to diabetes. *Am J Physiol Endocrinol Metab* 283: E423-E422, 2002

65. Yaspelkis BB, III, Davis JR, Saberi M, Smith TL, Jazayeri R, Singh M, Fernandez V, Trevino B, Chinookoswong N, Wang J, Shi ZQ, Levin N. Leptin administration improves skeletal muscle insulin responiveness in diet-induced inulin-resistant rats. *Am J Phisiol Endocrinol Metab* 280: E130-E142, 2001

66. Yaspelkis BB, III, Lessard SJ, Reeder DW, Limon JJ, Saito M, Rivas DA, Kvasha I, and Hawley JA. Exercise reverses high-fat diet-induced impairments on compartmentalization and activation of components of the insulin-signaling cascade in skeletal muscle. *Am J Physiol Endocrinol Metab* 293: E941-E949, 2007

67. Yaspelkis BB, III, Singh MK, Krisan AD, Collins DE, Kwong CC, Bernard JR, Crain AM. Chronic leptin treatment enhances insulin-stimulated glucose disposal in skeletal muscle of high-fat fed rodents. *Life Sci* 74: 1801-1816, 2004

68. Yip CC, and Ottensmeyer P. Three-dimensional structural interactions of insulin and its receptor. *J Biol Chem* 278: 27329-27332, 2003

69. Zierath JR, Houseknecht KL, Gnudi L, and Kahn BB. High-fat feeding impairs insulin-stimulated GLUT recruitment via and early insulin-signaling defect. *Diabetes* 46: 215-219, 1997

70. Zucker LM. Hereditary obesity in the rat associated with hyperlipemia. *Ann NY Acad Sci* 131: 447-458, 1965

71. Zucker LM and Antoniades HN. Insulin and obesity in the Zucker genetically obese rat "Fatty". *Endocrinology* 90: 1320-1329, 1972

72. Zucker LM, and Zucker TF. Fatty, a new mutation in the rat. *J Hered* 52: 275-278, 1961

73. Zucker TF, and Zucker LM. Fat accretion and growth in the rat. *J Nutrition* 80: 6-19, 1963

APPENDIX A

Immunoprecipitation

Solutions

2X Treatment Buffer (2X TB) (10 mL)

Reagent	Amount
4X Stacking gel Buffer	2.5 mL
10% SDS	4 mL
Glycerol	2 mL
Bromophenol Blue	2 mg
1 mM DTT	0.31 g

Add all reagents except Bromophenol Blue to a conical tube, pH to 6.8, add Bromophenol Blue and bring to volume with ddH_2O in a graduated cylinder. Store at -20° C.

Phosphate Triton Azide (PTA) Buffer (200 mL)

Reagent	Amount
Tween 20	1 mL
SDS	0.1 g
Sodium Azide	0.04 g
BSA	0.2 g

Add reagents to ~ 100 mL of ddH_2O in a beaker with a magnetic stir bar, pH to 7.2 and bring to volume with ddH_2O in a graduated cylinder.

Phosphate Buffered Saline (PBS) (500 mL)

Reagent	Amount
NaCl	4 g
KH_2PO_4	0.7 g
Na_2HPO_4	0.7 g
KCl	0.1 g

Add reagents to ~ 400 mL of ddH_2O in a beaker with a magnetic stir bar, pH to 7.4 and bring to volume with ddH_2O in a graduate cylinder.

Preparation of Protein-A (PRO-A) Sepharose Beads

1. Add 0.5 g of PRO-A sepharose (Amersham) to 10 mL of ddH_2O in a 15 mL test tube to swell the beads. Gently mix beads.
2. Place on rotator for 20 min at 4° C.
3. Centrifuge at 1,010 x g for 10 min at 4° C.
4. Discard supernatant and resuspend beads in an equal volume of ddH_2O. Gently mix beads.
5. Place on rotator for 20 min at 4° C.
6. Centrifuge at 1,010 x g for 10 min at 4° C.
7. Discard supernatant and resuspend beads in an equal volume of PTA. Gently mix beads.

8. Centrifuge at 1,010 x g for 10 min at 4° C.
9. Discard supernatant and resuspend beads in an equal volume of PTA. Gently vortex beads.
10. Using large orifice pipette tips, aliquot 1 mL of PRO-A beads into 1.5 mL screw top tubes. Gently vortex between each aliquot and store at -20° C.

Procedure

Day I

1. Prepare PRO-A beads.
2. Add 60 µL of PRO-A beads in a microcentrifuge tube.
3. Centrifuge beads at 13,000 x g for 2 min at 4°C.
4. Discard supernatant and add 180 µL of PBS to beads. Gently flick tubes to mix.
5. Centrifuge beads at 13,000 x g for 2 min at 4°C.
6. Repeat steps 4 and 5 twice.
7. Discard supernatant and add 150 µL of PBS and 4 µg of primary antibody to beads.
8. Incubate overnight at 4°C with rotation.

Day II

1. Centrifuge beads at 13,000 x g for 2 min at 4°C.
2. Discard supernatant and add 180 µL of PBS to beads. Gently flick tubes to mix.
3. Centrifuge beads at 13,000 x g for 2 min at 4°C.
4. Repeat steps 2 and 3 twice.

5. Discard supernatant and add 500 µg of protein. Gently flick tubes to mix.
6. Place samples on rotator for 2 h at 4°C.
7. Centrifuge beads at 13,000 x g for 2 min at 4°C.
8. Remove supernatant and keep in -80°C for later analysis.
9. Add 180 µL of PBS to beads. Gently flick tubes to mix.
10. Centrifuge beads at 13,000 x g for 2 min at 4°C.
11. Discard supernatant and add 180 µL of PBS with 2% Triton X to beads. Gently flick tubes to mix.
12. Centrifuge at 13,000 x g for 2 min at 4°C.
13. Discard supernatant and add 180 µL of PBS to beads. Gently flick tubes to mix.
14. Centrifuge beads at 13,000 x g for 2 min at 4°C.
15. Discard PBS, careful not to aspirate beads.
16. Add 25 µL of 2X TB to each sample and vortex.
17. Heat sample at 100°C for 5 min.
18. Samples can be either stored at -20°C or subjected to SDS-PAGE.

APPENDIX B

Sodium Dodecyl Sulfate-Polyacrylamide Gel Electrophoreses (SDS-PAGE)

Solutions

4X Resolving Gel Buffer (200 mL):

Reagent	Amount
Tris-Base	36.3 g

Add reagents to ~ 150 mL of ddH_2O in a beaker with magnetic stir bar, adjust pH to 8.8 and bring to volume with ddH_2O in a graduated cylinder.

4X Stacking Gel Buffer (50 mL)

Reagent	Amount
Tris-Base	3 g

Add reagents to ~ 40 mL of ddH_2O in a beaker with magnetic stir bar, adjust pH to 6.8 and bring to volume with ddH_2O in graduated cylinder.

10% SDS (100 mL)

Reagent	Amount
SDS	10 g

Add reagents to ~ 80 mL of ddH_2O in a beaker with magnetic stir bar and bring to volume with ddH_2O in a graduated cylinder.

10X Running Buffer (10X RB) (1 L)

Reagent	Amount
0.25 M Tris-Base	30.28 g
1.9 M Glycine	144.2 g

Add reagents to ~ 800 mL ddH_2O in a beaker with magnetic stir bar and bring to volume with ddH_2O in a graduated cylinder.

1X Running Buffer (1X RB) (1 L)

Reagent	Amount
10X Running Buffer	100 mL
10% SDS	10 mL
ddH_2O	890 mL

Add reagents in a beaker with magnetic stir bar.

10% Ammonium Persulfate (10% APS) (1 mL)

Reagent	Amount
APS	0.1 g
ddH_2O	1 mL

Add reagents to a 1.5 mL microcentrifuge tube and vortex.

Water Saturated N-Butanol (55 mL)

Reagent	Amount
N-Butanol	50 mL
ddH_2O	5 mL

Add reagents to a beaker and mix with a magnetic stir bar.

Polyacrylamide Resolving Gel Solution (4 Gels, 0.75 mm Thickness)

Reagent	7.5% Gel	10% Gel
Monomer Solution	5 mL	6.6 mL
4X Running Gel Buffer	5 mL	5 mL
10% SDS	200 µL	200 µL
ddH_2O	9.8 mL	8 mL
10% APS	100 µl	100 µl
TEMED	6.6 µL	6.6 µL

Add reagents to a conical tube and invert several times with a Pasteur pipette to mix.

Stacking Gel Solution (4 Gels, 0.75 mm Thickness)

Reagent	Amount
Monomer Solution	880 µL
4X Running Gel Buffer	1.67 mL
10% SDS	66 µL
ddH_2O	4.06 mL
10% APS	33.4 µL
TEMED	3.4 µL

Add reagents to a conical tube and invert several times with a Pasteur pipette to mix.

Procedure

1. Assemble gel apparatus according to the manufacturer's directions.
2. Prepare resolving gels.
3. Invert several times with a Pasteur pipette, avoiding bubbles. Fill caster approximately 3/4 full.
4. Overlay resolving gel with 500 µL of water saturated N-Butanol and allow gel to polymerize for approximately 1 h.
5. Pour N-Butanol off the resolving gel, rinse with ddH_2O and dry with Kimwipe.
6. Prepare stacking gel.
7. Invert several times with a Pasteur pipette, avoiding bubbles. Overlay resolving gel with stacking gel and insert combs. Allow approximately 45 min for polymerization.

8. Assemble gel apparatus chamber for electrophoresis according to manufacturer's directions.
9. Fill inner chamber with 1X RB and fill outer chamber approximately 1/4 full.
10. Load appropriate amount of sample protein.
11. Set the power supply at 200 V for 60 min.

APPENDIX C

Semi-Dry Transfer

Solutions

Transfer Buffer (1 L)

Reagent	Amount
48 mM Tris-Base	5.82 g
39 mM Glycine	2.93 g
10% SDS	3.75 mL
20% MeOH	200 mL

Add reagents to ~ 700 mL of ddH_2O in a beaker with magnetic stir bar and bring to volume with ddH_2O in a graduated cylinder. pH should range between 9.0 and 9.4. Do not adjust pH with acid or base.

10X Tris Buffered Saline (TBS) (1 L)

Reagent	Amount
200 mM Tris-Base	24.22 g
5 mM NaCl	292.2 g

Add reagents to ~ 800 mL of ddH_2O in a beaker with magnetic stir bar, pH to 7.5 and bring to volume with ddH_2O in a graduated cylinder.

Tween Tris Buffered Saline (TTBS) (1 L)

Reagent	Amount
10X TBS	100 mL
Tween 20	600 µL

Add reagents to ~ 800 mL of ddH_2O in a beaker with magnetic stir bar, pH to 7.5 and bring to volume with ddH_2O in a graduated cylinder.

Blocking Solution (20 mL)

Reagent	Amount
TTBS	20 mL
Non-Fat Dry Milk (NFDM) or Bovine Serum Albumin (BSA)	1 g

Add NFDM or BSA to TTBS and mix in beaker with magnetic stir bar. Need ~ 50 mL of blocking solution for each PVDF membrane.

Procedure

1. Following the completion of SDS-PAGE, separate resolving gel from gel plates and soak in transfer buffer for 30 min.
2. Soak polyvinylidene fluoride (PVDF) membrane in methanol for 30 s then soak in transfer buffer for 30 min.
3. Wet a sheet of blot paper in transfer buffer and place on the Trans-Blot electrode. Secure to electrode and roll out any air bubbles with a wet glass test tube.

4. Place PVDF membrane on top of blot paper and roll out any air bubbles with wet glass test tube. Pour a small amount of transfer buffer over PVDF membrane to avoid membrane from drying out.
5. Place resolving gel on top of PVDF membrane. Roll out any air bubbles.
6. Wet another sheet of blot paper in transfer buffer and place on top of resolving gel. Roll out any air bubbles with a wet glass test tube.
7. Set the power supply at 20 V for 30 min.
8. Following protein transfer, place PVDF membrane in approximately 50 mL of blocking solution. Block overnight at 4° C.

APPENDIX D

Immunoblotting

Solutions

IRS1 Primary Antibody (1:1,000) (40 mL)

Reagent	Amount
TTBS	40 mL
Polyclonal IRS1 Antibody (Cat# 06-526, Millipore)	40 µL
NaN_3	0.02 g
NFDM	0.40 g

aPKCζ/λ Primary Antibody (1:200) (50 mL)

Reagent	Amount
TTBS	50 mL
Polyclonal aPKCζ/λ Antibody (Cat# sc-216, SCBT)	250 µL
NaN_3	0.02 g
NFDM	0.50 g

GLUT4 Primary Antibody (1:1,000) (25 mL)

Reagent	Amount
TTBS	25 mL
Polyclonal GLUT4 Antibody (Donated by Dr. Cushman, NIDDK)	25 µL
NaN_3	0.0125 g
NFDM	0.25 g

IRS1 Secondary Antibody (1:10,000) (25 mL)

Reagent	Amount
TTBS	20 mL
Goat Anti-Rabbit (sc-2004, SCBT)	2 µl
NFDM	0.2 g

aPKCζ/λ Secondary Antibody (1:10,000) (25 mL)

Reagent	Amount
TTBS	20 mL
Goat Anti-Rabbit (sc-2004, SCBT)	2 µl
NFDM	0.2 g

GLUT4 Secondary Antibody (1:10,000) (20 mL)

Reagent	Amount
TTBS	20 mL
Goat Anti-Rabbit (sc-2004, SCBT)	2 µl
NFDM	0.2 g

Procedure

1. Following the overnight incubation with blocking solution, rinse membrane 2X in TTBS for 15 min.
2. Incubate membrane on primary antibody solution for 1.5 h on Lab Quake.
3. Recycle primary antibody and rinse membrane 2X in TTBS for 15 min.
4. Incubate membrane in secondary antibody solution for 1 h on Lab Quake.
5. Discard secondary antibody and rinse membrane 2X in TTBS for 15 min.

ADDENDIX E

Enhanced Chemiluminescence

Enhanced Chemiluminescence (ECL) (1.5 mL)

Reagent	Amount
Luminal/Enhancer Solution	1000 µL
Peroxide Buffer	500µL

Add solutions to 12 x 75 mm test tube and vortex.

Procedure

1. Prepare Visualizer Enhanced Chemiluminescence Substrate (Millipore).
2. Pour ECL solution directly on PVDF membrane and shake for 5 min.
3. Place PVDF membrane between two cut transparency and remove any air bubbles.
4. Turn on Chemi Doc system (BioRad, Richmond, CA) and select Quanty One Software on Macintosch G4 computer Chemi Doc system (BioRad).
5. Place PVDF membrane on Chemi Doc tray.
6. Select "auto expose" to acquire image.
7. Capture and save image.
8. Using the Quantity One Software, select "free hand contour tool" to quantify bands.
9. Select "volume analysis" to view data report.
10. Express samples as a percentage of the standard.

APPENDIX F

PI3 Kinase Assay

Solutions

PI 3-Kinase Homogenization Buffer (HB) (20 mL)

Reagent	Amount
1.0 mM HEPES	1 mL
100 mM Na-Pyrophosphate	4 mL
1.0 M β-Glycerophosphate	400 µL
0.5 N NaF	400 µL
100 mM Na_3VO_4	400 µL
80 mM EDTA	500 µL
10% IGEPAL	2 mL
100% Glycerol	2 mL
ddH_2O	7970 µL
100 mM PMSF	50 µL
0.4 M $MgCl_2$	50µL
0.5 M $CaCl_2$	40 µL
5 mg/mL Leupeptin	40 µL
1 mg/mL Aprotinin	200 µL

Add reagents to a conical tube, vortex and store at -20° C.

Phosphate Triton Azide (PTA) Buffer (200mL)

Reagent	Amount
Tween 20	1 mL
SDS	0.1 g
Sodium Azide	0.04 g
BSA	0.2 g

Add reagents to ~ 100 mL of ddH_2O in a beaker with a magenetic stir bar, pH to 7.2 and bring to volume with ddH_2O in a graduated cylinder.

"A" Wash (2500 µL)

Reagent	Amount
10% IGEPAL	125 µL
100 mM Na_3VO_4	2.5 µL
1mM DTT	2.5 µL
PBS	2370 µL

"B" Wash (2500 µL)

Reagent	Amount
1 M Tris-HCl	250 µL
2 M $LiCl_2$	625 µL
1 mM DTT	2.5 µL
100 mM Na_3VO_4	2.5 µL
ddH_2O	1620 µL

Add reagents to 12x75 mm glass test tube and vortex.

"C" Wash (5000 µl)

Reagent	Amount
1 M Tris-HCl	50 µL
NaCl	100 µL
10 mM EDTA	250 µL
1 mM DTT	5 µL
100 mM Na_3VO_4	5 µL
ddH_2O	45905 µL

Add reagents to a 13 x 100 mm glass test tube and vortex.

Dilute ATP

Reagent	Amount
ddH_2O	40 µL
50mM stock ATP	10 µL

ATP Solution (For 5 samples)

Reagent	Amount
ddH_2O	22.25 µL
0.4M $MgCl_2$	6.25 µL
4X HEPES Buffer	12.5 µL
Dilute ATP	1 µL

Add 8 µL ^{32}P in step 18 (day of use).

Preparation of Protein-A (PRO-A) Sepharose Beads

1. Add 0.5 g of PRO-A sepharose (Amersham) to 10 mL of ddH_2O in a 15 mL test tube to swell the beads. Gently mix beads.
2. Place on rotator for 20 min at 4° C.
3. Centrifuge at 1,010 x g for 10 min at 4° C.
4. Discard supernatant and resuspend beads in an equal volume of ddH_2O. Gently mix beads.
5. Place on rotator for 20 min at 4° C.
6. Centrifuge at 1,010 x g for 10 min at 4° C.

7. Discard supernatant and resuspend beads in an equal volume of PTA. Gently mix beads.
8. Centrifuge at 1,010 x g for 10 min at 4° C.
9. Discard supernatant and resuspend beads in an equal volume of PTA. Gently vortex beads.
10. Using large orifice pipette tips, aliquot 1 mL of PRO-A beads into 1.5 mL screw top tubes. Gently vortex between each aliquot and store at -20° C.

Procedure

Day I

1. Make sure there is enough HB to last through the tissue homogenization and the assay. It takes approximately 4 mL of HB to wash the beads for 9 samples.
2. Constantly check the amount of solutions available for use in this assay. Give special attention to the amount of [γ-^{32}P] ATP, and protein-A Sepharose beads, these get depleted very quickly.

Day II

1. Get ice, samples (store in -80°C freezer), antibody (antibody, Cat# 06-248, UBT), Protein-A Sepharose and HB (-20°C freezer) and thaw on ice. Run 9 samples plus a standard per assay. The volume of HB, anti-IRS-1, and sample are as follows: for each sample, add the following in a 500 µL microcentrifuge tube: volume of that corresponds to 250 µg of protein (based on Bradford assay), volume that correspond to 4 µg on anti-IRS-1, and bring to 125 µL with HB.

2. Quickly vortex, then pulse in mini microcentrifuge for 10 s each. Incubate samples on ice for 2 hours.
3. During the last 40 minutes of the 2 h incubation, set out solutions for the A, B, C washes, turn on the sonicator and refrigerated microcentrifuge and let cool to 4°C. Wash the Protein-A Sepharose beads by spinning thawed mixture for 3 min (4°C) at 14,000 rpm. Discard the supernatant and create a 1:1 dilution of HB to beads. Flick tubes to mix and centrifuge in a refrigerated microcentrifuge (14,000 rpm, 4°C) for 3 min.
4. Discard supernatant and add equal volume of HB to beads. Flick tubes to mix and spin in a refrigerated microcentrifuge (14,000 rpm, 4°C) for 3 min.
5. After spin is complete, discard the supernatant and add equal volume of HB to beads.
6. Using a cup pipette tip, add 80 μL of Protein-A beads to each sample. Vortex the beads between each addition. Rotate samples for 1.5 h at 4°C.
7. Set out 100mM sodium vanadate, 50mM ATP solution and 1M DTT(-20°C freezer) on ice.
8. Make the dilute ATP solution in a separate microcentrifuge tube labeled "DATP".
9. Make the ATP solution in another microcentrifuge tube labeled "ATP". Do not add the radioactive [γ-^{32}P] ATP yet.
10. *Preparation of the phosphatidylinositol (PI).* Prior to making the wash buffers, get a tube of PI from the -20°C freezer and place it under a light stream of air to evaporate. The evaporation should take approximately 7 min. After evaporating the PI, there should be a small white pellet at the bottom of the tube. Add 125 μL

of ice cold 4X HEPES and 375 μL of ice cold ddH_2O. Leave the PI out at room temperature and get a 40 mL beaker filled with ice water for use during sonication.

11. Now, label two 12x75 glass test tubes. One "A" and one "B". Label a 13x100mm glass test tube "C". Get 10 mL ddH_2O and place on ice. Dilute the 80mM EDTA (pH 8.0) (1:8) in a 1.5 mL microcentrifuge tube and label it "EDTA". A, B, and C washes should be made as follows:
12. The 1.5 h incubation should be near its end. Spin in a refrigerated microcentrifuge (14,000 rpm, 4°C) for 10 min.
13. *Sonication of PI*: This is done during each A, B and C wash spins. Apply parafilm to the microcentrifuge tube and vortex PI for one minute. Sonicate PI in ice water for one minute with bursts every three seconds. If PI becomes warm after each minute of sonication, increase the amount of time between each burst and make sure the ice water is freezing. If the temperature of PI becomes too warm, a conformational change of the lipid will occur rendering it useless. Perform sonication 15 times, vortexing PI for one minute every third minute of sonication.
14. When the 10 min centrifuge is complete take the samples out of the refrigerated microcentrifuge and discard the supernatant of each sample. Add 200 μL of wash buffer "A" and flick tube to mix. Centrifuge for 10 min. Continue to sonciate PI.
15. At the end of the "A" wash spin, take samples out of centrifuge and discard the supernatant. Add 200 μL of wash buffer "B" and flick tube to mix. Centrifuge for 10 min and continue to sonicate PI.

16. Discard supernatant, add 200 μL of wash buffer "C" and flick tubes to mix. Centrifuge spin in a refrigerated microcentrifuge (14,000 rpm, 4°C) for 10 min while continuing to sonicate PI. Make sure the entire supernatant is discarded as to mix washes during each of the spins.
17. Repeat step 16. At this point the sonication should be complete. Set out the washed tubes in a microcentrifuge tube rack and discard the supernatant. No more than one minute after the last sonication, add 20 μL of sonicated PI to each sample tube. If PI is not milky white color, DO NOT ADD TO SAMPLES. Vortex each sample intermittently for 7 min and place tubes behind the Plexiglass shield for the kinase reaction.
18. Add 600 μL of chloroform and 600 μL of MeOH to a 12x75 mm test tube, vortex thoroughly and set behind shield. Add 8 μL of [γ-^{32}P] ATP to "ATP" solutions, vortex and place behind shield.
19. Now get three pipettes and place behind shield. Set one at 10 μL for the addition of the [γ-^{32}P] ATP solution, another at 15 μL to stop the kinase reaction with 4 N HCl, and the third at 130 μL for the chloroform/MeOH. Add 10 μl of [γ-^{32}P] ATP solution (tube labeled "ATP") to the first sample tube, set timer and vortex for 20 sec. Continue this process for each sample tube. During the time between each addition of [γ-^{32}P] ATP solution, vortex samples periodically for 5 sec.
20. At 7.5 min, place first sample in a small microcentrifuge and pulse for 20 sec. At 8 min, stop the reaction in the first tube by adding 15 μL if 4 N HCl, quickly vortex, and add 130 μL of the chloroform/MeOH solution. Vortex for one

minute. Continue for all samples. *All samples must incubate for 8 min and not longer.*

21. Place samples in refrigerated microcentrifuge and spin (14,000 rpm, 4°C) for 3 min. During this spin, make the TLC Running Buffer. After 3 min, spin all samples, they should have three visible layers; a pink layer on top, the beads in the middle and the sample of interest at the bottom.

TLC Running Buffer

Reagent	Amount
Chloroform	74.81 mL
Methanol	58.60 mL
ddH_2O	14.09 mL
Ammonium Hydroxide	2.49 mL

22. Take a TLC plate and with the white side facing up, apply nine small pencile dots approximately 1 cm apart and 1 inch above the bottom of the TLC plate. Set the plexiglass shield, TLC plate, a pipette tip set at 20 μL, and the chloroform/MeOH solution inside of a working hood. Take samples out of the centrifuge and place them behind the shield as well. Pre-wet a pipette tip in the chloform/MeOH solution. Gently penetrate the top two layers of your sample tube and extract 20 μL of the bottom sample layer. On the first pencil dot, spot the TLC plate with the sample. Do not touch the TLC plate rather, use capillary action and make frequent contact. Use a light air stream to dry the spots so as not to make them

bigger than a pencil eraser. This allows for better migration of the sample. Again, pre-wet a new pipette tip, and extract 20 μL of sample and repeat the spotting process as stated above.

23. Fill the TLC tank with 130 mL of TLC Running Buffer. Fully open the fume hood door and gently place TLC plate inside of the tank. Allow the TLC buffer to run up the plate for 1 h.

24. After the 1 h separation of phophoinositides, take the TLC plate out of the tank and let it dry for 15 min. During this time, erase the Phosphor screen. Cover TLC plate with saran wrap and place inside a Phosphor imaging cassette, keeping orientation the same as spotting. After the Phosphor screen is erased, place it with the white side facing down on the TLC plate. Close the cassette and expose for a minimum of 3 h. Exposure time will vary depending on the age of the [γ-^{32}P] ATP.

25. Following the exposure, place the Phosphor screen into a Phosphor imager and generate an image of the Phosphor screen using a Quantity One, Personal FS software (BioRad). For each sample, you should be able to visualize a dark black spot on the bottom of the image, with a light straight line pointing up and ending with a distinct "V" pattern. The "V" pattern is your area of interest. Quantify the density of the "V" pattern using Quantity One (BioRad) software. Calculate each sample as a percentage of a standard that was spotted on the TLC plate.

APPENDIX G

aPKCζ/λ Kinase Activity Assay

Solutions

PKC Reaction Buffer (1 mL)

Reagent	Amount
50 mM Tris	50 µL
0.4 M $MgCl_2$	25 µL
1.0 mM ATP	40 µL
ddH_2O	885 µL

Add reagents in a microcentrifuge tube.

40% Acrylamide/Bisacrylamide (29:1) (100 mL)

Reagent	Amount
Acrylamide	38.66 g
Bisacrylamide	1.34 g

Add reagents to ~ 75 mL of ddH_2O in a beaker with magnetic stir bar, bring to volume with ddH_2O in a graduated cylinder and filter solution through 0.45 µm filter paper.

3X Tris-Tricine Gel Buffer (500 mL)

Reagent	Amount
Tris-Base	182 g
SDS	1.5 g

Add reagents to ~ 300 mL of ddH_2O in a beaker with magnetic stir bar, adjust pH to 8.45, bring to volume with ddH_2O in a graduated cylinder and filter through 0.45 μm filter paper.

1.5X Tris-Tricine Treatment Buffer (1.5X Tris/Tricine TB) (10 mL)

Reagent	Amount
Tris-HCl	2 mL
Glycerol	4 mL
10% SDS	2 mL
B-Mercaptoethanol	200 μL
Brilliant Blue	800 μL

Add all reagents to a conical tube and bring to volume with ddH_2O in a graduated cylinder.

50% Glycerol (20 mL)

Reagent	Amount
Glycerol	10 mL
ddH_2O	10 mL

Add reagents to a conical tube and vortex.

10X Tris-Tricine Running Buffer (10X Tris/Tricine RB) (1 L)

Reagent	Amount
Tris-Base	121.1 g
Tricine	179.2 g
SDS	10 g

Add reagents to ~ 800 mL of ddH_2O in a beaker with magnetic stir bar and bring to volume with ddH_2O in a graduated cylinder.

1X Tris-Tricine Running Buffer (1X Tris/Tricine RB) (1 L)

Reagent	Amount
10X Tris/Tricine RB	100 mL
ddH_2O	900 mL

Add reagents in a beaker with magnetic stir bar.

20% Tris-Tricine Resolving Gel (4 Gels, 0.75 mm Thickness)

Reagent	Amount
40% Acrylamide/Bis (29:1)	10 mL
3X Tris/Tricine Gel Buffer	6.6 mL
ddH_2O	1.4 mL
50% Glycerol	2 mL
10% APS	100 µL
TEMED	10µL

Add reagents to a conical tube and invert several times with a Pasteur pipette to mix.

Stacking Gel Solution (4 Gels, 0.75 mm Thickness)

Reagent	Amount
40% Acrylamide/Bis (29:1)	1 mL
3X Tris/Tricine Gel Buffer	3.3 mL
ddH_2O	5.7 mL
10% APS	50 µL
TEMED	10 µL

Add reagents to a conical tube and invert several times with a Pasteur pipette to mix.

Procedure

Day I

1. Prepare PRO-A beads as described in Appendix A.

2. Using a large orifice pipette tip, add 100 μL of PRO-A slurry in microcentrifuge tube.
3. Wash 3X with PBS as described in Appendix A.
4. After final wash, discard the supernatant and add 150 μL of PBS and 5 μg aPKCζ primary antibody (Cat# sc-216, SCBT).
5. Incubate overnight at 4°C with rotation.

Day II

1. Wash beads 3X as described in Appendix A.
2. After final wash, carefully discard the supernatant and add 100 μg of protein lysate in each microcentrifuge tube.
3. Place samples on rotator for 3 h at 4°C.
4. After incubation, centrifuge samples at 13,000 x g for 3 min at 4°C.
5. Remove supernatant and keep the sample in -80°C for later analysis.
6. Wash beads 3X with PBS as described in Appendix A.
7. Following the last wash, use gel loading tip to discard supernatant, careful not to aspirate beads.
8. Perform following reaction behind shield.
9. Add the following in order to each sample 30 μL PKC reaction buffer, 5 μL Myelin basic protein, and 0.5 μL [γ-^{32}P] ATP.
10. Vortex on heating block set at room temperature (37°C) for 12 min. rotating through samples on 20 sec intervals. Start 12 min timer after [γ-^{32}P] ATP has been added to the last sample.
11. Dilute sample 1:2 (1 part sample: 2 parts buffer) with 1.5X Tris Tricine buffer.

12. Denature samples on heating block set at 100°C for 5 min.
13. Store overnight in -20°C freezer in lab.

Day III

1. Assemble gel apparatus according to the manufacturer's directions.
2. Prepare 20% Tris-Tricine resolving gels.
3. Invert several times with a Pasteur pipette, avoiding bubbles. ill caster approximately ¾ full.
4. Overlay resolving gel with 500 µL of water saturated N-Butanol and allow gel to polymerize for approximately 1 h.
5. Pour N-Butanol off the resolving gel, rinse with ddH_2O and dry with Kimwipe.
6. Prepare stacking gel.
7. Invert several times with Pasteur pipette, avoiding bubbles. Overlay resolving gel with stacking gel and insert combs. Allow approximately 45 min for polymerization.
8. Assemble gel apparatus chamber for electrophoreses according to manufacturer's directions.
9. Fill inner chamber with 1X Tris-Tricine RB and fill outer chamber approximately ¼ full.
10. Load 5-10 µL (~ 7 µL) of sample to each lane.
11. Set the power supply at 100V for 130 min.
12. Approximately 15 min before electrophoreses is complete, erase the phosphor screen (Eastman Kodak Company).

13. Following completion of electrophoreses, separate Tris-Tricine resolving gel plates, remove stacking gel and cut resolving gel just above the dye front.
14. Place gels in cassette, cover with transparency and place white side of phosphor screen directly over transparency.
15. Expose gels to phosphor screen overnight.
16. Following the exposure, place the phosphor screen into the phosphor imager (Eastman Kodak Company) and generate and image of the phosphor screen using Quantity One Software on Macintosh computer.
17. Select "Personal FX" from file menu.
18. Select scan area by framing the appropriate coordinates.
19. Generate image using 200 μm resolution.

APPENDIX H

Raw Data for insulin-stimulated tissue

Group	Body Mass in grams	RQ-3MG Transport	RG-3MG Transport	PI3-K Activity	aPKCζ Cytoplasm	aPKCζ Plasma membrane
Lean	219.1	3.0	0.94	177.9442	65.68993	81.59743
Lean	224.1	4.8	0.99	136.8036	68.22643	82.01838
Lean	198.0	6.4	1.93	257.9637	73.772	82.98845
Lean	170.7	1.38	2.02	172.417	78.49023	87.93804
Lean	215.2	6.43	5.21	84.69531	79.07636	104.1835
Lean	230.0	3.91	2.25	220.7476	79.76833	112.9717
Lean	199.0	2.43	2.59	261.1028	82.712	133.6042
Lean	233.1	2.93	2.06	286.3618	82.73155	151.2605
Obese	347.7	3.13	1.72	21.02686	89.90903	44.73709
Obese	345.6	1.14	0.9	82.78271	101.1944	45.33314
Obese	364.1	0.59	0.91	71.32429	102.2335	54.35442
Obese	340.6	1.7	0.5	87.00231	108.2523	57.41151
Obese	387.7	2.18	1.85	92.48262	118.0699	69.06434
Obese	390.3	0.88	1.53	84.04179	118.0855	69.70624
Obese	435.1	0.94	0.64	39.30014	121.9298	79.92527
Obese	393.7	N/A	N/A	N/A	134.9352	80.39486

Group	aPKCλ Cytoplasm	aPKCλ Plasma membrane	aPKCζ/λ Activity Cytoplasm	aPKCζ/λ Activity Plasma membrane	GLUT4 Cytoplasm	GLUT4 Plasma membrane
Lean	74.27648	89.34966	157.6996	169.6806	61.44404	95.21391
Lean	89.8366	90.3214	181.8308	171.5384	45.81904	97.95417
Lean	95.57362	97.88519	219.7133	174.6373	48.68091	101.2559
Lean	93.99014	126.9935	238.1703	185.2986	63.79740	94.52656
Lean	92.29314	147.2025	291.8603	188.2594	49.01722	98.93107
Lean	116.5514	216.7255	310.186	209.1116	66.63867	105.4402
Lean	113.6616	86.55074	379.5263	213.4251	43.06671	97.26594
Lean	58.05113	88.01401	133.5087	247.094	74.25073	N/A
Obese	62.11725	41.31413	6.091177	71.36607	38.75777	65.3785
Obese	84.99263	48.71829	74.00777	92.31097	42.53407	69.43896
Obese	69.096	58.67962	85.61694	99.58145	47.36865	69.02138
Obese	61.84265	64.08412	88.81037	116.7597	29.98072	62.38535
Obese	70.1781	70.66153	95.82535	118.5758	28.02736	73.86625
Obese	64.56876	86.31431	131.6357	128.9748	20.01847	58.2039
Obese	41.64017	88.17699	138.4066	134.3831	36.09373	61.82569
Obese	39.19467	88.67073	142.1269	148.3779	N/A	69.15233

Raw Data for basal tissue

Group	Body Mass in grams	RQ-3MG Transport	RG-3MG Transport	PI3-K Activity	aPKCζ Cytoplasm	aPKCζ Plasma membrane
Lean	219.1	3.0	0.94	54.05832	39.41123	71.08187
Lean	224.1	4.8	0.99	46.18006	41.49328	75.34418
Lean	198.0	6.4	1.93	47.98161	48.52243	60.79022
Lean	170.7	1.38	2.02	55.32762	50.16159	76.28867
Lean	215.2	6.43	5.21	75.15598	59.78052	65.42769
Lean	230.0	3.91	2.25	63.23635	64.71198	64.72412
Lean	199.0	2.43	2.59	65.34053	66.40808	60.66309
Lean	233.1	2.93	2.06	71.48239	71.47343	100.1139
Obese	347.7	3.13	1.72	57.39274	40.14691	49.76069
Obese	345.6	1.14	0.9	65.70897	40.98196	41.49104
Obese	364.1	0.59	0.91	60.902	46.42167	45.13511
Obese	340.6	1.7	0.5	53.82735	46.85583	45.66894
Obese	387.7	2.18	1.85	71.03175	47.39355	44.90346
Obese	390.3	0.88	1.53	52.2512	47.75928	40.75893
Obese	435.1	0.94	0.64	50.4061	48.95279	50.12667
Obese	393.7	N/A	N/A	40.25078	50.10403	N/A

Group	aPKCλ Cytoplasm	aPKCλ Plasma membrane	aPKCζ/λ Activity Cytoplasm	aPKCζ/λ Activity Plasma membrane	GLUT4 Cytoplasm	GLUT4 Plasma membrane
Lean	49.69655	92.25766	150.8086	119.2871	76.29586	47.96190
Lean	46.83305	60.40633	155.7224	121.0649	82.4121	55.94291
Lean	52.67286	82.42443	159.0528	156.1711	65.80856	48.27324
Lean	51.42194	87.57303	163.2161	182.87	64.14498	49.59344
Lean	51.45164	75.77527	165.9362	32.81095	68.57939	52.21970
Lean	50.53445	70.06354	212.3884	69.53843	87.16169	52.54190
Lean	48.45585	103.9751	262.7768	79.92907	76.82226	41.46354
Lean	48.86948	N/A	497.6733	354.8252	83.41548	62.80154
Obese	49.84206	52.71122	36.08294	39.60939	55.00647	45.91561
Obese	48.0197	55.23837	88.67612	66.34257	44.27366	55.13351
Obese	49.46712	54.511	93.18777	70.37669	61.42655	54.23925
Obese	52.71523	50.12667	130.4642	72.01598	54.36815	56.70544
Obese	42.32278	52.20963	130.8728	80.60254	52.63821	54.57583
Obese	29.17253	26.09537	137.4511	84.66716	56.73507	61.31892
Obese	N/A	60.80089	203.5384	111.087	42.51893	56.27392
Obese	N/A	N/A	238.1056	208.5533	45.0447	59.36821